Widespread regulation of the maternal transcriptome by Nanos in Drosophila

mRNA regulatory targets of Nanos in Drosophila

Mohammad Marhabaie*, Tammy H. Wharton, Sung Yun Kim, and Robin P. Wharton#

#Corresponding author:
Department of Molecular Genetics
Department of Cancer Biology and Genetics
Center for RNA Biology
Ohio State University 484 W. 12th Avenue
Columbus, OH 43210

*Current address:
The Steve and Cindy Rasmussen Institute for Genomic Medicine
Abigail Wexner Research Institute at Nationwide Children's Hospital
Columbus, OH 43215

Abstract

The translational repressor Nanos (Nos) regulates a single target, maternal *hunchback* (*hb)* mRNA, to govern abdominal segmentation in the early Drosophila embryo. Nos is recruited specifically to sites in the 3'-UTR of *hb* mRNA in collaboration with the sequence-specific RNA-binding protein Pumilio (Pum); on its own, Nos has no binding specificity. Nos is expressed at other stages of development, but very few mRNA targets that might mediate its action at these stages have been described. Nor has it been clear whether Nos is targeted to other mRNAs in concert with Pum or via other mechanisms. In this report, we identify mRNAs targeted by Nos via two approaches. In the first method, we identify mRNAs depleted upon expression of a chimera bearing Nos fused to the nonsense mediated decay (NMD) factor Upf1. We find that, in addition to *hb*, Upf1-Nos depletes ~2600 mRNAs from the maternal transcriptome in early embryos. Virtually all of these appear to be targeted in a canonical, *hb*-like manner in concert with Pum. In a second, more conventional approach, we identify mRNAs that are stabilized during the maternal zygotic transition (MZT) in embryos from *nos*$^{-}$ females. Most (86%) of the 1185 mRNAs regulated by Nos are also targeted by Upf1-Nos, validating use of the chimera. Approximately 60% of mRNAs targeted by Upf1-Nos are not stabilized in the absence of Nos. However, Upf1-Nos mRNA targets are hypo-adenylated and inefficiently translated at the ovary-embryo transition, whether or not they suffer Nos-dependent degradation in the embryo. We suggest that the late ovarian burst of Nos represses a large fraction of the maternal transcriptome, priming it for later degradation by other factors during the MZT in the embryo.

54

55 **Introduction**

56 Nanos is a conserved cytoplasmic repressor that binds to mRNAs, recruiting
57 effectors that block translation and promote degradation (1,2). A wealth of genetic
58 evidence reveals that Nanos is primarily active in the germline, where it controls various
59 aspects of development in a number of organisms. In Drosophila, mouse, and humans,
60 Nos is required for the maintenance of germline stem cells (3–5). Later in germline
61 development, Nos regulates common pathways in the primordial germ cells (PGCs) of
62 Drosophila (6–9) and C. elegans (10,11), including the repression of somatic gene
63 transcription, inhibition of proliferation, and escape from apoptosis.

64 Evidence of a role for Nos in somatic cells is more limited. In the prospective
65 somatic cytoplasm, Nos has been thought to have one major regulatory target for
66 specification of abdominal segmentation, maternal *hb* mRNA (discussed below) (12–
67 14). At later stages of development, Nos regulates dendritic arborization in the
68 peripheral nervous system and the structure of the neuro-muscular junction of larvae
69 (15–17). In other somatic tissues, a latent capacity of Nos to regulate gene expression
70 is revealed in the absence of *lethal (3) malignant brain tumor* [*l(3)mbt*], which encodes a
71 component of two transcriptional repressor complexes (dREAM and LINT). In *l(3)mbt*
72 mutant larval brains and somatic ovarian cells, expression of Nos (and other germline-
73 restricted genes) is derepressed; remarkably, although hundreds of transcripts are
74 derepressed in the absence of *l(3)mbt*, mutant phenotypes in both tissues are
75 completely suppressed by loss of Nos activity (18,19). A similar latent regulatory
76 capacity of Nos has been identified in cultured mammalian cells lacking dREAM activity

77 (20). In Drosophila (and likely other organisms as well), both the expression of Nos in
78 the germline and its repression in somatic cells is important for normal development.
79 Given the diversity of its biological roles, it is likely that Nos regulates a number
80 of mRNAs in various organisms. Support for such an idea comes from the Seydoux lab,
81 who compared the maternal transcriptomes in wild type and *nos* mutant PGCs from
82 early C. elegans embryos, before the onset of zygotic transcription (10). They found
83 that levels of 171 maternal mRNAs are up-regulated in the absence of the redundant
84 function of both Nos-1 and Nos-2, which are required for normal development and
85 survival of the PGCs. It is unclear how many additional maternal mRNAs are
86 translationally repressed but not destabilized, and therefore undetected in their
87 experiments. Later in embryonic PGC development, 871 PGC mRNAs are up-regulated
88 in the absence of Nos function as a result of both delayed turnover of maternal mRNAs
89 and inappropriate zygotic transcription. Nos is not thought to directly regulate
90 transcription, and so presumably acts indirectly to stimulate accumulation of new,
91 zygotic mRNAs.
92 The mechanism of Nos-dependent regulation is best understood for repression of
93 maternal *hb* mRNA in Drosophila. On its own, Nos binds with high affinity but no
94 detectable sequence specificity to RNA (21,22); however, in collaboration with Pumilio
95 (Pum), it is recruited specifically to composite binding sites (Nanos Response Elements
96 , NREs) in the *hb* mRNA 3'-UTR (22,23). The composite sites have the consensus
97 sequence $\frac{U}{A}\frac{U}{A}\frac{U}{A}$UGUA, with Nos recognizing the first three degenerate positions and
98 Pum the next four. Within the Pum/Nos/RNA ternary complex, amino acid interactions
99 along a protein-protein interface mediate conformational changes in both proteins that

100 enhance binding. A key component of the interface is the Nos C-terminal tail, which is
101 essential for RNA binding; seven amino acids in the tail of the Nos^{L7} mutant protein are
102 absent, and as a result it is not recruited into a ternary complex and does not regulate
103 *hb* mRNA in the embryo (22–24).

104 Despite an atomic-level understanding of Nos recruitment to the *hb* NRE, two
105 outstanding questions about Nos activity in Drosophila remain. First, how many mRNAs
106 does Drosophila Nos regulate in addition to *hb* (and the handful referenced above)?
107 And second, is Nos recruited to other regulatory targets via its C-terminal tail in
108 collaboration with Pum, as has generally been assumed; or do other RNA-binding
109 proteins recruit Nos via a different mechanism? If Nos bound to a long, information-rich
110 sequence that were rigidly constrained, analysis of the transcriptome sequence might
111 be sufficient to identify likely regulatory targets. But the consensus NRE has low
112 information content and mutations in the NBS portion of the site have only a modest
113 effect on activity in vivo (25). So even though 6225 3'-UTRs in the total Drosophila
114 transcriptome bear one or more consensus NREs (26), it is unclear whether these are
115 genuine regulatory targets in vivo.

116 To address these issues, we first attempted to identify mRNAs that co-purify with
117 Nos, a method that has been used successfully to identify Pum targets, for example
118 (27,28). Initial reconstruction experiments revealed a disappointingly small enrichment
119 of *hb* mRNA. We therefore turned to an unconventional approach, expressing in flies a
120 protein with the Nonsense Mediated Decay (NMD) factor Upf1 fused to Nos. Early work
121 on NMD showed that tethering Upf1 via an exogenous RBD to a mRNA could direct its
122 degradation (29,30); we reasoned that tethering Upf1 to mRNAs via Nos might lead to

123 their degradation, and that Nos regulatory targets would be depleted from the
124 transcriptome in RNAseq experiments.
125
126 **Results**
127 As shown in Figure 1A, Nos is expressed at four important stages of oogenesis
128 and early embryogenesis (24,31,32): (1) in the germline stem cells (GSCs), where it is
129 required for maintenance of stem cell status; (2) in a high-level burst at stage 10B in the
130 nurse cells just prior to a general shutdown of transcription as the egg chamber nears
131 maturation; (3) during oogenesis stages 13-14 and continuing during syncytial nuclear
132 cleavage cycles 1-9 in a gradient emanating from the posterior pole of the embryo,
133 where it represses translation of maternal *hb* mRNA; (4) at nuclear cycle 10 in the
134 PGCs, where it regulates proliferation, blocks apoptosis, and is required for migration
135 into the somatic gonad much later in embryogenesis. After division of the GSC,
136 expression of Nos is turned off in the differentiating daughter cell (the cystoblast) and
137 subsequently re-expressed at various stages of oogenesis. No role has been ascribed
138 to Nos in these stages of oogenesis, including the burst at stage 10B.
139
140 **Figure 1 Upf1-Nos suppresses activity of anterior determinants *bicoid* and**
141 ***hunchback*.** A. Timeline of Nos expression during oogenesis and early
142 embryogenesis, focusing on four developmental stages. Note that nuclear cycle (nc) 10
143 occurs at ~ 90 minutes of embryonic development. The ~10-hour period of
144 transcriptional quiescence preceding harvesting of mRNA samples for subsequent
145 analysis is noted above. B. Embryonic phenotypes resulting from maternal expression

146 of the four regulatory proteins, as indicated. For the bargraph (note the logarithmic y-
147 axis), embryos were aged ≥ 24 hours (which allows wild type to hatch) and then scored
148 by sorting into three bins: cuticle with normal polarity (either hatched or not), cuticle with
149 anterior polarity inversion and a bicaudal body plan, or no cuticle (empty egg), which
150 includes both unfertilized eggs and embryos that die prematurely. C. The distribution of
151 *bcd* mRNA in Upf1-Nos and Upf1-Nos^{L7} embryos at two different stages of early
152 embryogenesis-- nuclear cycle (nc) 1 in the first two rows and nc 9 in the second two
153 rows. At each stage, two micrographs of a single embryo are shown, using Nomarski
154 optics to visualize *bcd* mRNA and morphology (above), and fluorescence methods to
155 visualize DAPI-stained DNA (below). Statistical analysis is reported in S1 Data. Note
156 that Upf1-Nos embryos appear to be unusually fragile during the fixation for in situ
157 hybridization; many are lost on the wall of the glass tube or at the heptane/aqueous
158 interface.

159 <u>Expression of Upf1-Nos inhibits activity of the anterior determinants Hb and Bicoid (Bcd)</u>
160 <u>and causes the degradation of *bcd* mRNA</u>

161 With the goal of identifying mRNA regulatory targets of Nos, we prepared
162 transgenic flies that express either a Upf1-Nos chimera, or one of three control proteins:
163 Upf1; Nos; or Upf1- Nos^{L7} , which bears the C-terminal tail deletion that abrogates
164 recruitment to *hb* mRNA. Transcription of each transgene is dependent on the GAL4
165 driver that is introduced by appropriate crosses, and each transgenic mRNA bears the
166 3'-UTR of wildtype *nos* mRNA to provide the post-transcriptional regulation conferred on
167 native *nos*.

168 We first drove expression of Upf1-Nos and the three control proteins described
169 above with Nos GAL4-VP16, which directs transcription in the germarium and
170 subsequent stages of oogenesis. Females expressing Upf1-Nos produce essentially no
171 eggs and bear rudimentary ovaries; in contrast, females expressing Upf1, Nos, or Upf1-
172 Nos^{L7} appear to produce normal numbers of eggs. As explained in more detail below,
173 we wished to harvest eggs at nuclear cycle 9 to take advantage of the prolonged
174 transcriptional quiescence flanking the oocyte-egg transition (Fig 1A), and therefore
175 asked whether use of other GAL4 drivers to direct expression of Upf1-Nos would permit
176 egg development. We found this to be the case with a maternal *alpha*Tub> GAL4
177 driver, which directs expression throughout much of oogenesis and was used in all
178 subsequent experiments.

179 Although females expressing Upf1-Nos lay eggs, virtually none hatch. In a small
180 pilot study, 0/245 Upf1-Nos eggs hatched, whereas between 80 and 95% of Upf1, Nos,
181 or Upf1-Nos Nos^{L7} control eggs hatched. Since expression of Upf1-Nos is exclusively
182 maternal, we expected that defects might be evident early in embryonic development.
183 Therefore we harvested 0-3 hour-old embryos and examined the distribution of nuclei
184 by staining with DAPI to assess developmental progress. Unlike the three control
185 genotypes, a large fraction of Upf1-Nos embryos have a single nucleus and are either
186 not fertilized or fail to commence nuclear division cycles; we have not investigated this
187 further, and restricted subsequent analysis to fertilized embryos between nuclear cycles
188 2-13. Almost all the Upf1, Nos, and Upf1-Nos Nos^{L7} embryos exhibit normal
189 distributions of syncytial cleavage stage nuclei (94% - 100%, see S1 Data for details).
190 In contrast, 63% of Upf1-Nos embryos have abnormal nuclear distributions, with

191 irregularly spaced nuclei and variable DNA content, based on the intensity of DAPI
192 fluorescence (e.g., Fig. 1C).

193 We next asked whether the Upf1-Nos embryos that fail to hatch exhibit
194 interpretable developmental defects by examining their body plan, as revealed by
195 pattern in the epidermal cuticle secreted late in embryonic development. 97% of Upf1-
196 Nos eggs were "empty," without detectable cuticle, probably because they die earlier in
197 development (Fig. 1B). However, among the 3% of Upf1-Nos embryos that did secrete
198 cuticle, 2 had normal segmentation and 14 revealed a striking bicaudal body plan, in
199 which normal head and thoracic segments are replaced by a mirror image duplication of
200 posterior abdominal segments (Fig. 1B). Bicaudal development is diagnostic for
201 simultaneous inhibition of Bcd and Hb activity (33–35). None (0/862) of the Upf1, Nos,
202 or Upf1-Nos Nos^{L7} control embryos exhibited segmental polarity reversals, much less a
203 mirror image duplication of the abdomen. As shown in Fig. 1B, most (80%-95%) of the
204 control embryos secreted cuticle that revealed body plans with normal antero-posterior
205 polarity and, at most, minor defects; the remaining embryos failed to secrete cuticle.

206 Even though only a few Upf1-Nos exhibited bicaudal body plans, the phenotype
207 is sufficiently characteristic to strongly suggest that Upf1-Nos inhibits activity of both Hb
208 and Bcd. *bcd* is transcribed exclusively maternally, while *hb* is transcribed both
209 maternally and later, zygotically (under the control of Bcd). For simplicity, we therefore
210 focused on examining the effects of Upf1-Nos on *bcd* mRNA by in situ hybridization in
211 early cleavage stage embryos. Most (82%) of the Upf1-Nos embryos that were either
212 unfertilized or in the first nuclear division cycles have a normal level of *bcd* mRNA at the
213 anterior (Fig. 1C); this was also the case for most (95%) control Upf1- Nos^{L7} embryos in

214 cycles 0-2. But we observed a novel phenotype in Upf1-Nos embryos that we judged to
215 be approximately in cycles 9-10 based on nuclear density: an absence of detectable
216 *bcd* mRNA (Fig. 1C). In contrast, Upf1- Nos^{L7} embryos in cycles 9-10 have normal
217 levels and distributions of *bcd* mRNA at the anterior pole.

218 In summary, the vast majority of control Upf1, Nos, and Upf1-Nos^{L7} embryos
219 develop normally, which is consistent with subsequent analysis of their transcriptomes
220 (below). In contrast, Upf1-Nos embryos are abnormal: many fail to either fertilize or
221 commence nuclear division, subsequent nuclear divisions are abnormal, only a handful
222 escape the deleterious early effects of Upf1-Nos and progress through to late
223 development, and none hatch. Most importantly, two phenotypes-- the absence of *bcd*
224 mRNA during early development and the bicaudal body plan of Upf1-Nos embryos--
225 support our premise that the chimeric protein would degrade Nos-regulated mRNAs.
226

227 <u>Upf1-Nos depletes 39% of maternal mRNAs</u>

228 To identify targets of Upf1-Nos in the entire transcriptome, we prepared triplicate
229 samples from 4 experimental embryos (Upf1, Nos, Upf1-Nos, Upf1-Nos^{L7}) as well as
230 wild type embryos as a control. Embryo collections were soft-fixed in methanol, stained
231 with DAPI, and manually sorted in the fluorescence microscope to identify embryos at
232 nuclear cycle 9-10, or in the case of Upf1-Nos, embryos that appeared to be
233 approximately the same age despite an abnormal distribution of nuclei (as in Fig. 1C).
234 Because transcription in the germ line ceases at stage 10B of oogenesis and resumes
235 only during the MZT (maternal zygotic transition) beginning at nuclear cycle 10, pre-
236 existing Upf1-Nos (or the other ectopically-expressed regulators) in the collected

237 embryos have had the opportunity to act on the maternal transcriptome for ~9-10 hours
238 without synthesis of new mRNA. Prior to the transcriptional "shutoff," Upf1-Nos might
239 cause changes to the transcriptome via both direct and indirect mechanisms; we hoped
240 that direct action of Upf1-Nos during the period of transcriptional quiescence would
241 have a predominant effect on transcriptome composition in embryos harvested at
242 nuclear cycle 9. RNA was prepared from all the genotypes, prepared for RNAseq, and
243 analyzed by standard methods.

244 We first assessed the quality of our samples. The absence of detectable mRNAs
245 encoded by genes that comprise the first zygotic response to maternal patterning
246 gradients (e.g., *Kr*, *gt*, *kni*) supports the idea that embryos were in fact collected prior to
247 the MZT (see S2 Data). Reducing the complexity of all 15 samples by Multi-
248 dimensional Scaling reveals that biological replicates are similar to each other and that
249 the control samples are also similar to each other (S1 Fig). In contrast, the Upf1-Nos
250 samples are markedly different from all three UAS controls and wild type, consistent
251 with their unusual embryonic phenotypes (Fig. 1).

252 We next compared the transcriptomes of each experimental genotype to wild
253 type to identify genes with altered expression, arbitrarily setting a minimum two-fold
254 threshold change and a FDR < 0.05. For simplicity, we describe data in which all
255 mRNA isoforms for a gene are binned; analysis of individual mRNA isoforms yields
256 broadly similar results (S2 Fig). We initially found that a small fraction of the maternal
257 transcriptome is depleted (2.4%) or enriched (2.1%) upon expression of Upf1 alone (Fig
258 2A). Because we were interested primarily in mRNAs that are targeted by the Nos

259 portion of the Upf1-Nos chimera, we excluded Upf1-regulated genes from subsequent
260 analysis of Upf1-Nos and Upf1- Nos^{L7}.
261
262 **Fig 2 Upf1-Nos targets a large fraction of the maternal transcriptome.** A. For
263 each of the mis-expressed proteins, the plot shows the difference in mRNA abundance
264 in comparison to wt (log_2 Fold Change) as a function of the average mRNA abundance
265 (log_2 Transcripts per Million reads) for embryonic samples collected at nc 9-10. Each
266 dot represents a binned collection of mRNA isoforms for a single gene; analysis of
267 individual isoforms is in S2 Fig. Genes altered by expression of Upf1 are excluded from
268 the analysis of Upf1-Nos and Upf1-Nos^{L7} data. Gene-binned mRNAs significantly
269 depleted and enriched are indicated in blue and orange, respectively. The green lines
270 mark $log_2 \pm 1$, and the figures at the right indicate the fraction of the (gene-binned)
271 transcriptome that is significantly changed and above or below the arbitrary twofold
272 cutoff. *hb* is highlighted in the Upf1-Nos plot. B. Correlation between the difference in
273 mRNA abundance (Upf1-Nos vs. wt) measured by RNAseq and by RT-qPCR for a
274 collection of genes, which span an ~1000-fold range in expression level in wt. C. The
275 results of DAVID analysis reveal gene sets enriched among Upf1-Nos-targeted mRNAs
276 (red) and non-targeted mRNAs (blue), which are plotted vs. their enrichment scores
277 (ES). Shown are annotation clusters with highest ES for which at least one Category
278 has a Benjamini adjusted p-value < 0.05. For clarity, three clusters that satisfy these
279 criteria and are enriched among non-targeted mRNAs with ES between 2.3 and 1.9
280 were omitted (see S2 Data for details). D. Examples of enriched gene sets, highlighted
281 on the Upf1-Nos vs. wt plot from A.

282

283 As shown in Fig 2A, the expression of Upf1, Nos, or Upf1- Nos^{L7} has relatively
284 little effect on the transcriptome. The proportion of significantly up- and down-regulated
285 genes is approximately the same for Upf1 and Nos, and the proportion of the
286 transcriptome depleted by Upf1- Nos^{L7} is only modestly greater than the proportion of
287 up-regulated genes. In striking contrast, >39% (n = 2596) of the genes encoding
288 maternal mRNAs are depleted more than twofold by Upf1-Nos. We note that the large,
289 asymmetric effect of Upf1-Nos on the transcriptome results in over-sampling of non-
290 targeted mRNAs; as a result we normalized the data using an average derived from 20
291 highly expressed mRNAs (most of which encode ribosomal proteins), as described in
292 Methods and S2 Data. To test the normalization and obtain an independent measure of
293 changes in abundance due to expression of Upf1-Nos, we measured the levels of 16
294 mRNAs by RT-qPCR; these were chosen to span a $\log_2$ = 15-fold change in
295 abundance. As shown in Fig. 2B, the two methods show excellent agreement, with a
296 Pearson's correlation R value of 0.98. The absence of a significant population of
297 enriched mRNAs in the Upf1-Nos data supports a premise of our experiment-- that
298 tethering Upf1 to mRNAs via Nos during the transcriptionally quiescent period preceding
299 sample collection would lead to their degradation via NMD and that this degradation
300 would predominate in shaping the composition of the transcriptome. We assume that
301 indirect effects (i.e., up-regulation of some mRNAs as a secondary consequence of the
302 action of Upf1-Nos on other, directly-targeted mRNAs) are minimized in the absence of
303 concurrent transcription.

304 Several observations support the idea that, although Upf1-Nos targets a large
305 portion of the transcriptome, it does so specifically. First, the inactivity of Upf1-Nos^{L7}
306 argues that the wild type chimera acts in collaboration with Pum to specifically target
307 NRE-bearing mRNAs, a point we return to in the following section. Second, three of the
308 four mRNAs previously shown to be bound and regulated by Nos-- *hb*, *bcd*, and *alpha-*
309 *Importin* (36,37)-- are targeted by Upf1-Nos; moreover, *hb*, which is the critical Nos
310 target in the early embryo, is one of the most highly depleted mRNAs (highlighted in Fig
311 2A). The exception is *CycB* mRNA, which is bound by Nos in collaboration with Pum
312 and repressed in the PGCs (1,7), but not targeted by Upf1-Nos. [We note that, for
313 reasons that are not clear, Nos is necessary but not sufficient to repress most of the
314 *CycB* mRNA in these experiments which derives from the prospective somatic
315 cytoplasm (1)]. Third, if Upf1-Nos acted promiscuously, due to high non-specific binding
316 (for example), it would preferentially target mRNAs with longer 3'-UTRs; in fact mRNAs
317 targeted by Upf1-Nos have on average slightly shorter 3'-UTRs than non-targeted
318 mRNAs (S3 Fig).
319 The depletion of such a large fraction of the transcriptome by Upf1-Nos suggests
320 that Nos may regulate thousands of mRNAs in Drosophila, in contrast to the hundreds
321 regulated by Nos in C. elegans (10). Since such a large fraction of the transcriptome is
322 targeted by Upf1-Nos, it is unclear whether it is meaningful to identify preferentially
323 targeted pathways. Nevertheless, clustering analysis of gene function via DAVID
324 (38,39) reveals that a number of pathways are significantly enriched among the pool of
325 genes targeted by Upf1-Nos as well as the pool of untargeted genes (Fig 2C). Among
326 Upf1-Nos targeted genes, only four clusters have gene subsets with significant

327 Benjamini-adjusted *p*-values; the most highly enriched of these subsets encodes factors
328 involved in DNA replication and repair (Enrichment Score [ES] = 3.1, Fig 2C), perhaps
329 accounting for the aberrant replication seen in Upf1-Nos embryos (Fig. 1C). An
330 independent search for Drosophila genes associated with the Gene Ontology terms
331 "DNA replication" and "DNA repair" revealed that 79/79 are depleted, as shown in Fig
332 2D. Among genes not targeted by Upf1-Nos, constituents of the ribosome (ES= 20.7)
333 and spliceosome (ES = 9.2) are even more significantly enriched (Figs 2C,D). We
334 conclude that while Upf1-Nos selectively targets a few biological processes/pathways
335 with modest preference, it acts globally to deplete maternal mRNAs that encode factors
336 distributed across most biological functions.
337
338 Upf1-Nos acts primarily in conjunction with Pum
339 Three lines of evidence support the idea that, in targeting a large fraction of the
340 maternal transcriptome, Upf1-Nos acts in collaboration with Pum, much as native Nos
341 and Pum collaboratively repress *hb* mRNA.
342 First, Upf1-Nos^{L7} is almost inert, changing the transcriptome to the essentially
343 same minor extent as does Upf1 (Fig 2A). The C-terminal tail of Nos that is altered in
344 the L7 mutant is specifically required to promote cooperative binding of Pum and Nos to
345 the NREs in *hb* mRNA.
346 Second, a set of 538 ovarian mRNAs that co-purify with affinity-tagged Pum (27)
347 is enriched among mRNAs depleted by Upf1-Nos [*p*-value = 0.03 by the CAMERA
348 competitive test of (40), Fig 3A].
349

Figure 3. Pumilio mediates most of the activity of Upf1-Nos. A. Barcode plot showing enrichment of mRNAs depleted by Upf1-Nos among the mRNAs bound by transgene-encoded Pum RNA-binding domain in ovarian extracts identified by Gerber et al. (2006). Each mRNA is represented by a line; mRNAs depleted and enriched > $\log_2$=1 are highlighted in blue and red, respectively. Here and in subsequent barcode analyses, the x-axis is non-linear. B. A modified NRE motif (shown above) is enriched among the 3'-UTR sequences of mRNAs depleted by Upf1-Nos. The plot below is of adjusted *p*-values (Hommel) for the significance of the enrichment on the y-axis of each motif variant displayed along the x-axis. Enrichment was calculated as described in the text, and each boxplot displays the distribution of *p*-values from 1000 trial comparisons between the fraction of 3'-UTRs bearing a motif in targeted vs. non-targeted mRNAs. C. Local regression analysis displays the density of NRE variants at position +4 in 3'-UTR sequence plotted against the $\log_2$ (Fold Change) in Upf1-Nos vs. wt (e.g., Fig 2A). Here and in subsequent local regression analyses, the x-axis is non-linear, light shading marks 95% confidence windows, the light dashed line marks $\log_2 = 0$, and the heavier dashed lines mark $\log_2 \pm 1$. Tests of whether the various NRE derivatives are more abundant among targeted 3'-UTRs (one-sided Wilcoxon) yield the following *p*-values: (U or A) < 2.2e-16, (A) 5.4e-07, (U) < 2.2e-16, (G) 0.057, (C) 1.

Third, the 3'-UTRs of mRNAs targeted by Upf1-Nos are enriched for a modified Nos+Pum binding motif, $\frac{U}{A}\frac{U}{A}\frac{U}{A}UGU\frac{U}{A}$, in which position +4 is either U or A. Several observations support this conclusion. We first asked whether the canonical Nos+Pum motif ($\frac{U}{A}\frac{U}{A}\frac{U}{A}$UGUA) is enriched among 3'-UTRs targeted by Upf1-Nos, comparing the

373 fraction of 3'-UTRs bearing the motif between targeted mRNAs and randomly selected
374 subsets of non-targeted mRNA (chosen to have the same number of sequences and a
375 similar distribution of 3'-UTR lengths). As shown at the far right of Fig 3B, the fraction of
376 targeted 3'-UTRs bearing a canonical site is significantly greater than the fraction of
377 non-targeted UTRs (median *p*-value of 1000 trials = 1.9e-05). As controls we asked
378 whether singly-substituted mutant derivatives at each of the seven motif positions are
379 also enriched. All of the derivatives but one appear to be "mutant" sites not significantly
380 enriched in targeted 3'-UTRs; the exception is $\frac{U}{A}\frac{U}{A}\frac{U}{A}$UGUU which, in fact, is enriched to
381 a greater extent than the canonical site (Fig 3B). We next determined that the average
382 number of modified Nos+Pum motifs is greater among 3'-UTRs targeted by Upf1-Nos
383 than among non-targeted 3'-UTRs (*p*-value < 12.2e-16 by Wilcoxon rank sum test).
384 Finally, localized regression analysis graphically reveals a correlation between the
385 density of $\frac{U}{A}\frac{U}{A}\frac{U}{A}UGU\frac{U}{A}$ sites in the 3'-UTR and the extent of depletion by Upf1-Nos (Fig
386 3C). All of these observations are consistent with work described elsewhere showing
387 that Nos+Pum bind efficiently to NREs with either U or A at position +4 (41).
388 Taken together, the evidence described above supports the idea that Upf1-Nos is
389 primarily recruited to its targets by Pum in a manner similar to their joint recruitment to
390 the *hb* NRE. We were unable to test Pum dependence directly, as *pum* mutant flies that
391 also express Upf1-Nos are subviable, and females produce very few eggs.
392
393 <u>Upf1-Nos may be recruited to a minor fraction of its targets by Bruno</u>
394 Although Upf1-Nos^{L7} is largely inactive (as described above), a small cohort of
395 178 genes is depleted > twofold upon expression of this mutant chimera. Localized

396 regression analysis reveals no significant correlation between the density of NREs and
397 the extent of depletion (Fig 4A, *p*-value = 0.087 by Wilcoxon test), and thus depletion is
398 unlikely to be the result of inefficient recruitment of the mutant Nos moeity to NREs via
399 Pum. We therefore considered the possibility that another RNA-binding protein might
400 recruit Upf1-Nos ^{L7} to this minor fraction of the transcriptome.
401
402 **Figure 4. Upf1-Nos targets a small portion of the transcriptome via Bruno.** A.
403 Similar to Fig 3C, local regression analysis displays the density of BRE and NRE sites
404 in 3'-UTR sequence plotted against the $\log_2$ (Fold Change) in Upf1-Nos^{L7} vs. wt (e.g.,
405 Fig 2A). Statistics for enrichment among mRNAs depleted > 2-fold reported in the text.
406 B. Barcode enrichment plot displaying mRNAs de-repressed upon inhibition of Bru
407 expression in the ovary (42) plotted vs. the $\log_2$ (Fold Change) in Upf1-Nos^{L7} vs. wt
408 (e.g., Fig 2A). C. DAVID analysis reveals enrichment of gene sets among mRNAs
409 targeted by Upf1-Nos^{L7}. D-F. Yeast interaction assays show that both Nos and Nos^{L7}
410 can be recruited to RNA-bound Bru. In each panel, the binding of AD-fusions to various
411 factors (y-axis) to a bait (title above each bargraph) is measured in arbitrary light units of
412 β-galactosidase (x-axis, $\log_{10}$ plot). For the "control" entry in each bargraph, yeast were
413 transformed with plasmids that express the bait indicated in the title and an empty
414 vector encoding AD only; the background level of β-galactosidase is also indicated with
415 a dashed line. D. Two-hybrid experiments showing protein-protein interactions
416 between Nos and Bru (above) and Bru and Nos (below). We are unable to assess
417 interaction with DBD fused to the Nos NTD, as the resulting fusion "auto-activates"
418 transcription of the reporter without an AD-fusion partner. E. Three-hybrid experiments

419 showing specific binding of Bru to RNA bearing wt BREs. Below the horizontal dashed
420 line is an additional control showing no significant binding of Bru to NREs. F. Four-
421 hybrid experiments showing binding of Nos and Nos^{L7} to Bru-bound RNA. Below the
422 horizontal dashed line are additional controls showing no binding of Nos in the absence
423 of Bru to RNA bearing either wt or mutant BREs. Note that the background level of β-
424 galactosidase is higher in the yeast strain used for 2-hybrid experiments than in the
425 strain used for 3- and 4-hybrid experiments.
426
427 To identify such a putative novel Nos co-factor, we used the DREME tool (43) to
428 search for motifs overrepresented among 3'-UTR sequences of mRNAs depleted by
429 Upf1-Nos^{L7}. The search revealed enrichment of the motif UAU $\frac{A}{U}$ U $\frac{G}{A}$ UA, which is
430 similar to one of the binding sites for Bruno: the Bruno Response Element (BRE) U $\frac{A}{G}$ U
431 $\frac{G}{A}$ U $\frac{A}{G}$ U (44). Localized regression analysis further shows that mRNAs depleted ≥
432 twofold by Upf1-Nos^{L7} are enriched in BREs (Fig 4A, *p*-value < 2.2e-16 by Wilcoxon
433 rank sum test).
434 Bruno (Bru) is a translational repressor that binds a number of RNA motifs via its
435 three RNA recognition motifs (RRMs) (45). mRNA regulatory targets of Bru in the ovary
436 have been identified by virtue of increased polysome association following RNAi-
437 mediated inhibition of Bru expression (42). If Bruno mediates the depletion of mRNAs
438 by Upf1-Nos^{L7} in our experiments, we would expect significant overlap with the Bru-
439 regulated mRNAs identified by Rangan and colleagues. This is indeed the case:
440 mRNAs depleted by Upf1-Nos^{L7} are enriched for Bru-regulated targets (*p*-value = 7.2e-
441 6, CAMERA competitive test), as revealed in a barcode enrichment plot (Fig. 4B).

442 Functional clustering of gene analysis reveals a number of enriched gene sets among
443 Upf1-Nos^{L7} targets; these encode membrane cytoskeleton factors or regulators (PDZ,
444 SH3, pleckstrin domain proteins, spectrin repeat proteins), at least one of which (β-
445 spectrin) plays a key role in GSCs and differentiation of their progeny (Fig 4C and S3
446 Data).

447 We next asked whether Bru can recruit Nos and Nos^{L7} to RNA. Previous
448 experiments have shown that Nos and Bru proteins interact (46,47). To further
449 characterize the Bru-Nos interaction, we performed yeast two-hybrid experiments, the
450 results of which are shown in Fig 4D. We find that a fragment of Bru interacts with full-
451 length Nos, stimulating LacZ reporter activity to a slightly greater extent than does
452 interaction with either of two known Nos effectors, Cup and NOT4 (Fig 4D above)
453 (1,48). In reciprocal experiments with DNA-binding domain (DBD) and transcriptional
454 activation domain (AD) fusions swapped, we observe binding of both Nos and Nos^{L7} to
455 Bru, demonstrating that the Bru-Nos interaction does not depend on an intact Nos C-
456 terminal tail. Consistent with this observation, Bru interacts with the Nos N-terminal
457 domain (NTD) but not its C-terminal RBD (Fig 4D below).

458 To directly test whether RNA-bound Bru can recruit Nos to RNA, we next used
459 yeast three-hybrid RNA-binding experiments to show that Bru binds specifically to a
460 synthetic RNA sequence with 3 copies of the canonical BRE, but not to RNAs with
461 either 3 copies of a mutant BRE or 2 copies of a NRE (Fig 4E). Then in yeast four-
462 hybrid experiments similar to those used to show Pum-dependent recruitment of Nos to
463 NREs (23), we find that RNA-bound Bru can recruit either Nos or Nos^{L7} to the RNA (Fig
464 4F). Recruitment is dependent on both the NTD and RBD of Nos, raising the possibility

465 that protein-protein interactions between Bru and Nos as well as protein-RNA
466 interactions between Nos and the RNA are required for formation of the ternary
467 Bru/Nos/RNA complex.

468 Although we initially identified Bru as a mediator of the activity of Upf1-Nos^{L7}, the
469 interaction experiments in Fig 4 (D-F) show that Bru does not interact specifically with
470 the L7 mutant form of the protein but also to a similar extent with wild type Nos. It
471 therefore seems likely that Bru mediates targeting of the same small subset of mRNAs
472 by both Upf1-Nos^{L7} and Upf1-Nos, but that Pum-mediated targeting of the much larger
473 set of mRNAs by the latter obscures the contribution by Bru. Consistent with this idea,
474 neither BREs (*p*-value = 0.129 by Wilcoxon rank sum test) nor Bru-repressed mRNAs
475 (*p*-value = 0.084 by CAMERA competitive test, S4 Fig) are enriched among mRNAs
476 targeted by Upf1-Nos.

477 In summary, we have shown that Bru can recruit Nos or Nos^{L7} to specific RNA
478 sequences, supporting the idea that Bru mediates targeting of a minor subset of the
479 maternal transcriptome by Upf1-Nos^{L7} (and presumably contributing to depletion of the
480 same minor subset by Upf1-Nos). The mechanism by which the Nos-Bru-BRE complex
481 forms is independent of the integrity of the Nos C-terminal tail and thus different from
482 cooperative binding of Nos+Pum to the *hb* NRE.

483

484 <u>mRNAs targeted by Upf1-Nos in transgenic animals are repressed in wildtype ovaries</u>
485 <u>and embryos by Nos</u>

486 We next asked whether mRNAs depleted by Upf1-Nos might be regulated by
487 endogenous Nos in wildtype animals. As a first step to addressing this question, we re-

488 analyzed two studies of maternal mRNAs in late oogenesis and early embryogenesis,
489 partitioning these into mRNAs either targeted or not targeted by Upf1-Nos.
490 In the first study, Lipshitz, Smibert, and colleagues (49) identified maternal
491 mRNAs that are degraded in unfertilized eggs; by definition, the regulation they
492 observed occurs in the absence of zygotic gene expression. Tadros et al. (2007)
493 identified 1069 mRNAs whose abundance drops at least 1.5-fold as unfertilized eggs
494 age. This set of destabilized maternal mRNAs is significantly enriched among our Upf1-
495 Nos targets (*p*-value = 1.6e-11; Fig 5A). The embryos used in their experiments were
496 unfertilized but otherwise wildtype, and therefore destabilization must be mediated by
497 endogenous maternal factors.
498
499 **Figure 5. Maternal mRNAs targeted by Upf1-Nos are translationally repressed**
500 **and degraded in wild type eggs.** A. Barcode plot displaying enrichment of maternal
501 mRNAs degraded in unfertilized eggs (49) vs. $\log_2$ (Fold Change) in Upf1-Nos vs. wt
502 (e.g., Fig 2A). B. Maternal mRNAs expressed at nc 9-10 in the RNAseq experiments of
503 Fig 2 were binned into those targeted (red) and not targeted (teal) by Upf1-Nos. Then,
504 the poly(A) tail length and relative translational efficiency of each mRNA was extracted
505 from the data of Eichorn et al. (2016) at the four stages of development indicated below:
506 stage 11 and 14 oocytes, activated eggs, 0-1 hr embryos (before the onset of zygotic
507 transcription). The plot at the right is of the change in abundance for each maternal
508 mRNA between each of the three developmental transitions indicated below, again
509 using the data of Eichorn et al. (2016). Statistical analysis in S4 Data. Note that zygotic
510 transcription contributes significantly to mRNA abundance in the 2-3 hr embryo pool, but

511 all other timepoints analyze purely maternal mRNAs. C. Local regression analysis of
512 binding motifs in mRNA 3'-UTRs as a function of Translational Efficiency (TE) at egg
513 activation, from the data of Eichorn et al. (2016). For this analysis, we chose the most
514 highly expressed maternal isoform for each gene.
515
516 In the second study, Bartel, Orr-Weaver, and colleagues (50) characterized
517 mRNAs in staged samples from wildtype ovarian egg chambers and timed embryo
518 collections up to 6 hours after egg deposition, measuring abundance, poly(A) tail length,
519 and translational efficiency (TE). Their work reveals comprehensive changes to the
520 maternal transcriptome during an extended span of development that includes the
521 oocyte-egg transition (e.g., the vertical dashed line in Fig 1A) and the maternal-zygotic
522 transition (MZT), a period from approximately 1.5-3.0 hours of embryonic development
523 during which many maternal mRNAs are degraded and zygotic transcription is
524 activated. (For reference, the MZT begins shortly after nuclear cycle 10 in Fig 1A.)
525 Analyzing their data, we find that mRNAs targeted by Upf1-Nos are regulated
526 differently than are non-targeted mRNAs. Non-targeted maternal mRNAs undergo
527 lengthening of their poly(A) tails at egg activation and concomitant enhanced
528 translation, consistent with the observation that poly(A) tail length and TE are coupled
529 until the onset of gastrulation (which occurs at 3 hours of embryonic development) (50).
530 In contrast, Upf1-Nos targets undergo neither poly(A) tail lengthening nor translational
531 enhancement (Fig 5B). The repressed Upf1-Nos targets are stable until later in the
532 MZT (2-3 hours of development), when they are preferentially degraded (Fig 5B). The

533 data likely underestimate the extent of degradation during the MZT, since some
534 maternally transcribed mRNAs are re-transcribed zygotically, as discussed below.
535 Taken together, the data in Fig 5 suggest that, late in oogenesis, the large set of
536 ~2600 mRNAs targeted by Upf1-Nos (in transgenic animals) is translationally repressed
537 in wild type animals during late oogenesis and degraded 2-3 hours later, during the
538 MZT. We suggest that these regulatory events are a delayed response to the burst of
539 Nos expression at stage 10B of oogenesis (Fig 1A), which represses targeted mRNAs
540 and primes them for subsequent degradation in the embryo.
541 As a first test of the idea that Nos is responsible for repressing a large cohort of
542 maternal mRNAs, we asked whether the modified NRE motif that mediates Nos+Pum
543 binding is over-represented among maternal mRNAs that are translated inefficiently at
544 egg activation. As shown in Fig 5C, localized regression analysis reveals a correlation
545 between the translational efficiency and the density of modified NRE motifs in the 3'-
546 UTR across the maternal transcriptome. In comparison with the 3'-UTRs of mRNAs that
547 are not repressed, the modified NRE is enriched in the 3'-UTRs of repressed mRNAs
548 (defined as TE < 1, *p*-value = 1.1e-8 by two-sided Wilcoxon test). As controls,
549 canonical Pum binding sites and BREs are both present at lower density (Fig 5C) and
550 are less enriched in repressed mRNAs (*p*-values of 7.3e-6 and 0.22, respectively).
551 All the work described above is based on the ectopic expression of Upf1-Nos,
552 which behaves like a hyperactive version of Nos that efficiently degrades bound
553 mRNAs. Part of the rationale for using Upf1-Nos is that, in the Drosophila embryo, Nos
554 acts primarily to block translation and only secondarily to promote the degradation of
555 targeted mRNAs (35,36,51,52). In C. elegans, RNAseq analysis of *nos* mutant PGCs

556 successfully identified a cohort of maternal mRNAs that are destabilized by Nos in wt
557 PGCs (10). This observation led us to ask (1) if we could detect Nos-dependent
558 destabilization of maternal mRNAs, and (2) whether the same mRNAs are targeted by
559 Upf1-Nos and by Nos. To address these issues, we collected embryos from wild type
560 and *nos*$^-$ females at 0-1 and 2-3 hours of development (i.e., before and after the onset
561 of zygotic transcription, respectively), and measured the abundance of maternal mRNAs
562 via RNAseq. In analyzing the data, we ignored mRNAs that are transcribed zygotically
563 but not maternally, since these are not exposed to and thus cannot be regulated by
564 Nos.

565 As shown in Fig 6A, at 0-1 hrs, the wt and *nos*$^-$ mRNA populations are similar in
566 composition, with only 3.5% of the maternal transcriptome significantly enriched
567 $>\log_2=0.5$-fold in *nos*$^-$ embryos. A somewhat greater fraction of the maternal
568 transcriptome (5.6%) is depleted in *nos*$^-$ embryos at this stage of development,
569 presumably due to indirect effects of Nos on gene expression earlier, during ovarian
570 development (since Nos is thought to act primarily as a repressor). However, after the
571 onset of the MZT, 18.5% of the maternal transcriptome is stabilized or up-regulated in 2-
572 3 hr *nos*$^-$ embryos (Fig 6A). A rank-ordered barcode display of mRNAs stabilized in the
573 absence of Nos reveals a correlation with mRNAs targeted by Upf1-Nos (*p*-value =
574 3.8e-14, Fig 6B left). In fact, 86% (1019/1185) of the mRNAs stabilized in the absence
575 of Nos are depleted by Upf1-Nos (Fig 6B middle). Taken together, the complementary
576 loss- and gain-of-function results of Figures 6 and 2 indicate that Nos regulates at least
577 these 1019 common mRNA targets.
578

579 **Figure 6. Regulation of maternal mRNAs by endogenous Nos in wild type**
580 **oocytes and embryos.** A. Results of RNAseq analysis, comparing the abundance of
581 maternal mRNAs between wild type and *nos*$^-$ embryos at 0-1 and 2-3 hr of embryonic
582 development. Only maternal mRNAs (based on the manually sorted embryos used in
583 the RNAseq experiments of Fig 2) are shown. The green lines mark $\log_2 \pm 0.5$, and the
584 figures at the right indicate the fraction of the (gene-binned) transcriptome that is
585 significantly changed and above or below the arbitrary cutoff, which is smaller than the
586 2-fold cutoff used in Fig 2 since the magnitude of destabilization by Nos is generally
587 smaller than the magnitude of degradation by Upf1-Nos. mRNAs stabilized or
588 destabilized in the absence of Nos at an FDR < 0.05 are orange and blue, respectively.
589 B. The barcode (left) shows mRNAs depleted by Upf1-Nos (Fig 2) plotted vs. the $\log_2$
590 (Fold Change) in *nos*$^-$ vs. wt at 2-3 hr (e.g., Fig 6A). Each depleted mRNA is a
591 hashmark, the length of which indicates the extent of depletion by Upf1-Nos; this plot
592 shows a poor correlation between the extent of degradation by Upf1-Nos and by Nos (in
593 wt embryos; see also the scatterplot to the right). The Venn diagram (middle) shows
594 that most of the maternal mRNAs stabilized in the absence of Nos are degraded by
595 Upf1-Nos. The scatterplot (right) shows the correlation between the extent of
596 degradation by Upf1-Nos and stabilization in the absence of Nos. The canonical Nos
597 substrate *hb* mRNA is highlighted as an extreme example, in which zygotic re-
598 expression between 2-3 hrs almost completely obscures Nos-mediated regulation of
599 maternal *hb* mRNA. In all these comparisons we analyze only the 6399 mRNAs
600 common to the two datasets (e.g., Figs 2A and 6A). C. Maternal mRNAs were divided
601 into three pools: down in Upf1-Nos and up in *nos*$^-$ at 2-3 hrs (Pool A = the 1019 mRNAs

602 of the Venn diagram above); down in Upf1-Nos only (Pool B = the 1528 mRNAs of the
603 Venn diagram), the remaining 3852 maternal mRNAs untargeted by Upf1-Nos (Pool C).
604 These bins were used to parse the data of Eichorn et al. (2016), as described for Fig 5.
605 Statistical analysis in S5 Data.
606
607 What then of the 1528 maternal mRNAs that are regulated by Upf1-Nos but
608 apparently not by Nos (Fig 6B middle)? One possibility is that they are repressed but
609 not degraded by Nos. Another possibility is that they are repressed and degraded by
610 Nos, and then re-expressed zygotically during the 2-3 hour window of embryonic
611 development. At this stage, Nos is confined to the PGCs (which constitute only a small
612 fraction of the volume of the embryo), and therefore essentially no zygotically re-
613 expressed mRNAs will suffer regulation by Nos even if they might be susceptible. This
614 is not a confounding issue for our analysis of Upf1-Nos activity, since mRNA was
615 harvested before the onset of transcription. However, zygotic re-expression likely does
616 mask regulation of mRNA stability by Nos, thereby accounting, at least in part, for the
617 modest correlation between the extent of regulation by Upf1-Nos and by Nos (R^2 = 0.25,
618 Fig 6B right). For example, the canonical Nos target *hb* (highlighted in the scatter plot in
619 Fig. 6B), which is among the most sensitive Upf1-Nos targets, is re-transcribed in the 2-
620 3 hr window such that the net level of *hb* mRNA at 2-3 hrs of development is not
621 significantly different in the presence or absence of Nos.
622 To estimate the potential influence of zygotic re-expression on the 2-3 hr
623 samples ± Nos, we analyzed data from Eisen and colleagues (53). Their
624 measurements of RNA abundance in precisely staged single embryos allows us to

625 determine the fraction of maternal mRNAs in our experiments that are re-expressed
626 zygotically within three pools: mRNAs targeted by both Upf1-Nos and Nos (pool A;
627 105/1019 = 10%); mRNAs targeted by Upf1-Nos but not Nos (pool B; 655/1528 = 43%);
628 mRNAs targeted by neither (pool C; 760/3852 = 20%). There is a striking enrichment of
629 zygotically re-expressed mRNAs in pool B (*p*-values < 2.2e-16 vs. pools A or C,
630 respectively, by Fisher's exact test). Taken together, these observations support the
631 idea that, for many of the genes in pool B, Nos-dependent degradation of the maternal
632 mRNA component might be masked by new transcription at 2-3 hrs. of embryonic
633 development (e.g., as for *hb*).

634 We reasoned that we might observe a reduction in poly(A) tail length and TE of
635 the 1528 mRNAs in pool B at earlier stages of development, before the potentially
636 confounding contribution of zygotic transcription. To test the idea, we returned to the
637 resource described by Eichorn et al. (2016), examining the fate of maternal mRNAs at
638 various stages from late oogenesis through the first hour of embryonic development.
639 Data were parsed into the three pools described above: (A) the 1019 mRNAs targeted
640 both by Upf1-Nos and Nos, (B) the 1528 mRNAs targeted only by Upf1-Nos, and (C)
641 the remaining 3852 mRNAs not targeted by Upf1-Nos. As shown in Fig 6C, the two
642 pools containing Upf1-Nos-targeted mRNAs (A and B) are regulated in a similar fashion,
643 particularly at egg activation: mRNAs in both pools are translationally repressed and
644 suffer shortening of their poly(A) tails (albeit, to slightly different extents, S5 Data). In
645 contrast, the mRNAs not targeted by Upf1-Nos (pool C) are translationally activated and
646 undergo lengthening of their poly(A) tails.

647 Overall, we conclude that, at or around the oocyte-egg transition, endogenous
648 Nos likely regulates most of the maternal mRNAs targeted by Upf1-Nos.
649

650 **Discussion**

651 The main conclusions from the work presented above are that Nos regulates
652 thousands of mRNAs in the maternal transcriptome and likely does so in concert with
653 Pum, binding jointly to NRE sequences much as they do to the canonical NREs in *hb*
654 mRNA. The latter idea is supported primarily from the relative inactivity of Upf1-Nos^{L7},
655 which bears a defective C-terminal tail, a critical element of the intricate set of protein-
656 protein and protein-RNA interactions that support formation of the Nos/Pum/*hb* NRE
657 ternary complex. In theory, the Nos C-terminal tail might mediate similar interactions
658 with another RNA-binding partner too. Although we cannot rule out such an idea, the
659 enrichment of NREs among mRNAs depleted by Upf1-Nos (Fig 3) or repressed at egg
660 activation (presumably by endogenous Nos, Fig 5) support the idea that most of the Nos
661 tail-dependent activity is mediated via Pum as a partner.

662 A number of factors drove us at the outset to adopting the unconventional
663 approach of using Upf1-Nos to target the transcriptome. First, we failed to achieve
664 meaningful enrichment of *hb* mRNA in pulldown experiments from embryonic extracts
665 expressing epitope-tagged Nos. This disappointing observation was mitigated by the
666 modest enrichment of the canonical Nos+Pum targets *hb* or *bcd* mRNA in the Pum
667 pulldown experiments of others (27,28). In these experiments, *hb* and *bcd* mRNA were
668 enriched only between 2- and 3.5-fold, even though Pum on its own is a high-affinity,
669 high-specificity binding protein. Given the modest enrichment for known Pum-bound

670 mRNA targets, the high non-specific binding activity of Nos, and our insignificant
671 enrichment of *hb* in pilot experiments, we were not encouraged to believe that we would
672 be able to purify other, less stable Nos complexes formed on suboptimal NREs, for
673 example. We also considered using UV-crosslinking to stabilize Nos/mRNA complexes
674 in extracts; but crosslinking of the purified Nos RBD is inefficient (23). In contrast, in
675 vivo expression of Upf1-Nos allowed us to achieve high activity and specificity: *hb* and
676 *bcd* are depleted 131- and 34-fold, respectively, by Upf1-Nos, whereas upon expression
677 of Upf1-Nos^{L7} *hb* is depleted only 1.5-fold and the level of *bcd* is not significantly
678 changed. The large dynamic range of our experiment allowed the identification of
679 thousands of less-sensitive targets, and over 1000 of these are verified by virtue of
680 stabilization in the absence of Nos (Fig 6). Nevertheless, a caveat to the present work
681 is that we have not shown that mRNAs regulated by either Upf1-Nos or Nos in vivo are
682 directly bound by Nos in vitro. Nor have we identified specific sites within regulated
683 mRNAs that mediate Nos action.

684 Although we have not identified the sites within regulated mRNAs that mediate
685 Nos (or Upf1-Nos) action, analysis of the population of targeted mRNAs has shown that
686 Nos+Pum preferentially recognize mRNAs with both UGUU and UGUA motifs. We
687 observe a correlation between the density of such motifs in the 3'-UTR and sensitivity to
688 Upf1-Nos, but have not been able to identify similar correlations between the total
689 number of motifs or their position within the 3'-UTR. At one level this is surprising, since
690 a single site is sufficient to confer regulation either in flies or in cultured cells, and the
691 degree of regulation correlates roughly with the number of sites (22,37). Therefore, one
692 might expect that mRNAs with many sites would be more sensitive, as the probability of

693 occupancy by a Nos+Pum repressor complex would be greater. This is clearly not the
694 case; for example, of the ten mRNAs in the transcriptome with the largest number of 3'-
695 UTR UGUA motifs (26), only one is targeted by Upf1-Nos. The correlation that we do
696 observe (Fig 3C) is consistent with the idea that higher site density promotes
697 cooperative interactions among nearby bound complexes. This model is supported by
698 experiments described elsewhere showing that the N-terminal domain of Pum interacts
699 with itself (Wharton et al., 2023). Finally, the contribution of other RNA-bound
700 regulators or RNA structure is too complex to currently be taken into account when
701 considering the entire transcriptome, as has been pointed out previously (26).

702 Given the large number of regulated mRNAs, it is not surprising that expression
703 of Nos protein is tightly controlled. During oogenesis and embryogenesis, much of this
704 control is exerted via the 3'-UTR of its mRNA to control the timing and location of protein
705 accumulation (31,54,55); we therefore intentionally designed all of the transgenes used
706 in this work to express mRNAs bearing the native *nos* 3'-UTR. Our results suggest an
707 additional level of control-- negative autoregulation. Nos mRNA is significantly
708 depleted (6.7-fold) by Upf1-Nos, and most of this regulation appears to be Pum-
709 mediated (e.g., only 1.3-fold depletion by Upf1-Nos^{L7}). The idea of negative
710 autoregulation is consistent with earlier work on the activity of Nos at the neuromuscular
711 junction, which hinted at Pum-dependent auto-regulation via non-canonical sites in the
712 *nos* 3'-UTR (16).

713 Based initially on analysis of the low residual activity of Upf1-Nos^{L7}, we argue
714 above that Bru may recruit Nos (or Nos^{L7}) to regulate a minor portion of the maternal
715 transcriptome. Such a model could explain an intriguing aspect of Nos biology in the

716 female germline stem cell and its progeny cystoblast, which differentiates into the cyst
717 of 16 cells that ultimately forms the germline component of each egg chamber. In
718 females bearing near-complete loss-of function *nos* alleles (e.g., nos^{RC}), GSCs are
719 specified normally but fail to maintain stem cell status following division: both daughter
720 cells differentiate and the ovary is rapidly denuded of its germline (56). However, GSC
721 function is maintained in the nos^{L7} mutant, suggesting that at least some of the essential
722 Nos function at this stage is tail-independent and therefore not mediated by Pum (24).
723 Our results are consistent with the idea that Bru mediates part of the activity of Nos in
724 early oogenesis, and does so whether the Nos C-terminal tail is intact or not. Bru is
725 required both early in the larval gonad for normal development of the GSCs in the larval
726 ovary and of their cystoblast progeny in the adult ovary (57). The definitive cellular
727 marker for the GSC and the cystoblast is the spectrosome, an unusual intracellular
728 sphere containing cytoskeletal proteins usually associated with the cellular membrane--
729 alpha- and beta spectrin, spectraplakin (which links actin and microtubule filaments),
730 and an adducin (encoded by *hts*), which mediates interactions between spectrin and
731 actin (58–60). We find that the mRNAs encoding these proteins and functionally related
732 cytoskeletal factors are enriched among Upf1-Nos^{L7} targets (Fig 4C). Taken together,
733 these observations lead us to speculate that at least part of the function of Nos in
734 maintaining stem cell identity in the GSCs may rely on Bru-mediated regulation of
735 mRNAs encoding the spectrosome and other cytoskeletal components.

736 Part of the motivation for identifying novel Nos regulatory targets was the hope of
737 gaining insight into its evolutionarily conserved role in the GSCs, where it maintains
738 stem cell identity by unknown pathways, and the PGCs, where it regulates proliferation,

739 contributes to selectively blocking transcription of somatic genes, and promotes escape
740 from apoptosis. The large number of Nos targets we have identified suggest it is
741 unlikely that Nos controls a single mRNA to maintain the GSCs in a manner similar to
742 the singular regulation of maternal *hb* mRNA that drives abdominal patterning in the
743 embryo. Translation is globally repressed in human hematopoeitic stem cells (61);
744 perhaps Nos-mediated global repression contributes to maintenance of a semi-dormant
745 state that promotes GSC maintenance. Alternatively, targeting of particular pathways
746 could regulate GSCs. For example, our finding that DNA replication gene mRNAs are
747 preferentially targeted by Upf1-Nos might depress fork speed, which has recently been
748 shown to promote a totipotent state in mouse embryonic stem cells (62). Upf1-Nos
749 preferentially spares ribosomal protein mRNAs, perhaps so that, following GSC cell
750 division, the cystoblast daughter (in which Nos drops to a low level) can immediately
751 commence differentiation. In addition, it is intriguing that Upf1-Nos spares proteins that
752 regulate mRNA biology (e.g., those encoding RRM proteins), given the importance of
753 post-transcriptional regulation in the GSC in particular and the germline in general.
754 Further work will be required to determine whether any of this regulation contributes to
755 GSC (or PGC) biology.

756 We initially analyzed the effects of Upf1-Nos on the maternal transcriptome at nc
757 9-10 largely because the preceding period of transcriptional quiescence provided a
758 convenient method of analyzing post-transcriptional effects on mRNA levels in the
759 absence of new synthesis. However, our findings suggest an unanticipated role for the
760 burst of Nos expression at stage 10B of oogenesis, just prior to the transcriptional
761 shutoff. Turnover of part of the maternal transcriptome is an essential aspect of

762 embryonic development in Drosophila. Degradation is controlled by a number of factors
763 (including Smg, Brat, ME31B, and mir-309; reviewed by (63) in successive waves
764 during syncitial embryonic development. Our finding that mRNAs targeted by Upf1-Nos
765 and/or Nos are preferentially hypo-adenylated and translationally repressed at egg
766 activation (Fig 6) is consistent with the idea that Nos contributes to this degradative
767 regulatory network. We favor the idea that the high level burst of Nos expression at
768 oogenesis stage 10B represses thousands of mRNAs, priming them for further
769 subsequent repression in the embryo by other factors and, ultimately, degradation. In
770 theory, the nascent posterior gradient of Nos, which initially forms at oogenesis stage,
771 could contribute as well. But given the difference in Nos protein levels at stages 10B
772 and 13-14 (31), we favor a model in which the stage 10B burst is responsible for most of
773 the coordinated regulation of poly(A) tail length, translational efficiency, and stability that
774 is observed. In this scenario, Nos is responsible for regulating mRNA fate on two very
775 different scales in the early embryo-- repressing a single mRNA (*hb*) to govern
776 abdominal segmentation and thousands of mRNAs to help direct turnover of the
777 maternal transcriptome.
778

779 **Materials and methods**

780 <u>Drosophila strains and methods</u>

781 Plasmids used in this study are described in S6 Data. Transgenic lines were
782 constructed by microinjection of w^{1118} embryos by standard methods. The following
783 strains were used: w^{1118} as the wild type reference in RNAseq experiments; the
784 maternal alpha-tubulin GAL4-VP16 driver (stock # 7062 from the Bloomington

785 Drosophila Stock Center [BDSC]); trans-heterozygotes of *nos*^{BN} and Df(3R)Exel6183
786 (stock # 7662, [BDSC]) for the RNAseq experiment of Fig. 6. We initially tested 3 or
787 more transgenic lines with the GAL4-VP16 driver for each construct, and observed only
788 minor phenotypic differences among the 3 lines. We screened for lines expressing
789 Upf1-Nos and Upf1-Nos^{L7} at essentially the same level by harvesting total RNA from
790 collections of 0-2 hr embryos and measuring the chimeric mRNA by RT-qPCR using the
791 appropriate primer pair in S2 Data. Fly stocks were maintained by standard methods
792 and grown at 25°C. Embryos were collected on apple-juice agar plates smeared with
793 yeast paste.

794 Early embryos for assessment of nuclear morphology (Fig 1) were prepared by
795 dechorionating in bleach, harvesting by filtration, fixing in 4% formaldehyde under
796 heptane for 20-30 minutes, removal of the aqueous phase and shocking into methanol.
797 Embryos were then rehydrated into phosphate-buffered saline (PBS) containing 0.1%
798 Tween-20 (PBT), and incubated with 5 µg/ml 4′,6-diamidino-2-phenylindole (DAPI) for
799 10 minutes, washed repeatedly with PBT, mounted in PBST containing 25% glycerol,
800 and examined by epifluorescence using a Zeiss Axiophot.

801 Embryonic cuticle was examined by harvesting embryos from apple juice plates
802 24 hours after removing adults, dechorionating with bleach, and mounting in
803 Hoyers/lactic acid. Slides were cleared by heating for several hours and then examined
804 by dark field microscopy using a Zeiss Axiophot.

805 In situ hybridization was performed essentially as described (64), with probe
806 prepared by nick translation of a double-stranded PCR product bearing the *bcd* ORF
807 using alkali-stable digoxigenin-11-2'-deoxyuridine-5'-triphosphate (Roche), visualizing

808 with alkaline-phosphate coupled sheep anti-digoxigenin Fab fragments (Roche) and
809 subsequent reaction with 5-bromo-4-chloro-3-indolyl phosphate and nitro blue
810 tetrazolium before examination using Nomarski optics on a Zeiss Axiophot.

811 For hand-sorting of embryos to identify those in nc 9-10, we followed the protocol
812 of (65) with the following modifications. Embryos were dechorionated in 100% bleach
813 for 1 minute, rinsed well, and then simultaneously devitellinized and fixed in a 1:1 ratio
814 of ice-cold methanol and heptane for 5 minutes with gentle rocking. The vials were
815 vortexed for 30 seconds, heptane and embryos at the interface removed, and the
816 remaining embryos washed with ice-cold methanol 3 times. Embryos were then
817 rehydrated into PBT with washing for 10 minutes and then stained with 0.1 µg/ml DAPI
818 for 10 minutes. After washing in PBT, embryos were sorted under UV illumination using
819 a Leica MZFLIII stereomicroscope.

820

821 RNAseq and RT-qPCR

822 Total RNA was extracted from sorted embryos using TRIzol reagent (Thermo
823 Fisher Scientific). Samples were submitted to the Ohio State University Cancer Center
824 Genomics Shared Resource for poly(A) selection and library preparation with TruSeq
825 (Illumina) and subsequently sequenced on a HiSeq4000 (Illumina) sequencer. Paired-
826 end 150-nucleotide raw reads were first processed and demultiplexed at the sequencing
827 facility, and subsequently processed as follows. Adapter sequences were trimmed
828 followed by trimming low-quality bases from the 3' end of reads based on a minimum
829 Phred score of 15. Reads of less than 60nt were removed, as were reads mapping to
830 mtRNA, tRNA, and rRNA. STAR (v2.5.3a) was used to map the reads either to the fly

831 genome or the transcriptome (Dobin et al., 2013). Mapped reads were counted using
832 RSEM (v1.3.0) (Li and Dewey, 2011). The resulting outputs were analyzed in R (v4.2.1)
833 using the edgeR package (v3.40.2) to find differentially expressed genes and transcripts
834 (Robinson et al., 2010). Low abundance genes and transcripts were filtered out by
835 setting min.count=30 and min.total.count=30 in filterByExpr function in the edgeR
836 package, removing genes and transcripts with < ~2 counts per million mapped reads.
837 All statistical analyses including differential expression and Locally Estimated
838 Scatterplot Smoothing (LOESS) were performed using R (v4.2.1).

839 To account for over-sampling caused by the large depletion of mRNAs targeted
840 by Upf1-Nos, correction factors were calculated as follows. We assumed that the most
841 abundantly expressed mRNAs, which are transcribed from housekeeping genes, are
842 not regulated by Upf1-Nos and thus can be used to calculate a correction factor. Rather
843 than relying on a single highly expressed gene (e.g., eEF1α1), an average correction
844 factor was calculated using the 20 most abundantly expressed genes for each Upf1-Nos
845 replicate. Among genes with the highest average read abundance in wild type samples,
846 we selected 20 with a similar rank order among Upf1-Nos and wild type samples. For
847 each gene, the ratio of read abundance in the Upf1-Nos replicate to its average
848 abundance across the three wild type replicates was calculated. The resulting ratios for
849 all 20 genes were averaged, yielding a correction factor for the replicate (S2 Data).
850 These correction factors were used as normalization factors for the Upf1-Nos replicates
851 in edgeR. A similar approach was used to calculate three correction factors for the
852 analysis of individual transcripts (S2 Data).

853 For RT-qPCR, cDNA was synthesized from 250 ng RNA using random hexamers
854 and qPCR performed using SYBR Green using a 7500 Real Time PCR machine
855 (Applied Biosystems). Triplicate measurements for each primer pair were obtained (for
856 each of the three biological replicates). Abundance of each RT product was calculated
857 relative to the abundance of RT product from RpS2 mRNA. Primer efficiencies for all
858 primer pairs were 90%-100%.
859
860 Motif enrichment analysis
861 Motif enrichment analysis was done using the following DREME command:
862 "dreme -rna -norc -png -e 0.1 -m 10 -o DEOUT -p input.fa". Parameters were set per the
863 user manual. To prevent outlier large 3'-UTRs (e.g., the ~10.5 kb *headcase* 3'-UTR)
864 from biasing the analysis, only UTRs <2600 nt (98% of all 3'-UTRs) were analyzed.
865
866 Gene ontology enrichment analysis
867 GO enrichment analysis was performed using DAVID (v6.8) with the default
868 setting and categories (COG_ONTOLOGY, UP_KEYWORDS, UP_SEQ_FEATURE,
869 GOTERM_BP_DIRECT, GOTERM_CC_DIRECT, GOTERM_MF_DIRECT,
870 KEGG_PATHWAY, INTERPRO, SMART).
871
872 Yeast interaction assays
873 Yeast were transformed with the 2μ plasmids described in Fig. 1 Supplement 1
874 by a standard lithium acetate/PEG protocol. For 2-hybrid experiments, we used the
875 PJ69-4A strain (66), which is *MAT**a***, *trp1-901*, *leu2-3*, *112*, *ura3-52*, *his3-200*, *gal4*Δ,

876 *gal80*Δ, *LYS2::GAL1-HIS3*, *GAL2-ADE2*, *met2::GAL7-lacZ*. Double transformants were
877 obtained and grown on minimal SD dropout medium lacking tryptophan and leucine.
878 For 3- and 4-hybrid experiments, we used the YBZ1 strain (67), which is *MAT**a**, ura3-*
879 *52, leu2-3, 112, his3-200, trp1-1, ade2, LYS2::(LexAop)-HIS3, ura3::(lexA-op)-lacZ,*
880 *LexA-MS2 coat (N55K)*. For 3- hybrid experiments, double transformants were grown
881 on minimal SD dropout medium lacking uracil and leucine, and for 4-hybrid experiments
882 triple transformants were grown on SD dropout medium lacking uracil, leucine, and
883 tryptophan.

884 β-galactosidase activity was measured using Beta-Glo (Promega) essentially as
885 described by Hook et al., 2005. Briefly, transformants were grown by diluting saturated
886 overnight cultures into appropriate selective media to early-log phase (OD_{600} = 0.2 -
887 0.3), and then 40 µl of culture was incubated with the same volume of Beta-Glo reagent
888 for 60 minutes at room temperature in 96-well microplates. Three transformants were
889 grown separately and assayed for each experiment. Samples were analyzed in a
890 Veritas luminometer (Turner Biosystems Inc). The output signal from the luminometer
891 was divided by the OD_{600} to normalize for the number of cells in each sample, and by
892 1000 (by convention) to generate a reading of beta-galactosidase activity in arbitrary
893 light units.

894

895 **Acknowledgements**

896 We thank Drs. K Panda, RK Slotkin, and R Bundschuch for advice and helpful
897 discussions, Dr. P Yan for assistance with RNAseq sample preparation, Drs. G Singh
898 and M Kearse for comments on the manuscript, H. Lipshitz for kindly forwarding their

899 data for analysis in Fig. 5A, and Dr. C Croce for encouragement and support. We
900 acknowledge services of the OSUCCC Genomics Shared Resource which is supported
901 by P30CA016058. Some fly stocks were obtained from the Bloomington Drosophila
902 Stock Center (NIH P40OD018537). This research was supported in part by NIGMS
903 R01GM084376 (RPW).

904

905 **Author ORCIDs**

906 RPW 0000-0001-8506-1379

907 MM 0000-0002-5609-2915

908 SYK 0009-0002-5624-9377

909

910 **References**

911 1. Kadyrova LY, Habara Y, Lee TH, Wharton RP. Translational control of maternal Cyclin B mRNA by
912 Nanos in the Drosophila germline. Dev Camb Engl. 2007 Apr;134(8):1519–27.

913 2. Raisch T, Bhandari D, Sabath K, Helms S, Valkov E, Weichenrieder O, et al. Distinct modes of
914 recruitment of the CCR4-NOT complex by Drosophila and vertebrate Nanos. EMBO J. 2016 May
915 2;35(9):974–90.

916 3. Kusz-Zamelczyk K, Sajek M, Spik A, Glazar R, Jędrzejczak P, Latos-Bieleńska A, et al. Mutations of
917 NANOS1, a human homologue of the Drosophila morphogen, are associated with a lack of germ
918 cells in testes or severe oligo-astheno-teratozoospermia. J Med Genet. 2013 Mar;50(3):187–93.

919 4. Tsuda M, Sasaoka Y, Kiso M, Abe K, Haraguchi S, Kobayashi S, et al. Conserved role of nanos
920 proteins in germ cell development. Science. 2003 Aug 29;301(5637):1239–41.

921 5. Wang Z, Lin H. Nanos maintains germline stem cell self-renewal by preventing differentiation.
922 Science. 2004 Mar 26;303(5666):2016–9.

923 6. Asaoka M, Sano H, Obara Y, Kobayashi S. Maternal Nanos regulates zygotic gene expression in
924 germline progenitors of Drosophila melanogaster. Mech Dev. 1998 Nov;78(1–2):153–8.

925 7. Asaoka-Taguchi M, Yamada M, Nakamura A, Hanyu K, Kobayashi S. Maternal Pumilio acts together
926 with Nanos in germline development in Drosophila embryos. Nat Cell Biol. 1999 Nov;1(7):431–7.

927 8. Kobayashi S, Yamada M, Asaoka M, Kitamura T. Essential role of the posterior morphogen nanos for
928 germline development in Drosophila. Nature. 1996 Apr 25;380(6576):708–11.

929 9. Sato K, Hayashi Y, Ninomiya Y, Shigenobu S, Arita K, Mukai M, et al. Maternal Nanos represses
930 hid/skl-dependent apoptosis to maintain the germ line in Drosophila embryos. Proc Natl Acad Sci U S
931 A. 2007 May 1;104(18):7455–60.

932 10. Lee CYS, Lu T, Seydoux G. Nanos promotes epigenetic reprograming of the germline by down-
933 regulation of the THAP transcription factor LIN-15B. eLife. 2017 Nov 7;6.

934 11. Subramaniam K, Seydoux G. nos-1 and nos-2, two genes related to Drosophila nanos, regulate
935 primordial germ cell development and survival in Caenorhabditis elegans. Dev Camb Engl. 1999
936 Nov;126(21):4861–71.

937 12. Hülskamp M, Schröder C, Pfeifle C, Jäckle H, Tautz D. Posterior segmentation of the Drosophila
938 embryo in the absence of a maternal posterior organizer gene. Nature. 1989 Apr 20;338(6217):629–
939 32.

940 13. Irish V, Lehmann R, Akam M. The Drosophila posterior-group gene nanos functions by repressing
941 hunchback activity. Nature. 1989 Apr 20;338(6217):646–8.

942 14. Struhl G. Differing strategies for organizing anterior and posterior body pattern in Drosophila
943 embryos. Nature. 1989 Apr 27;338(6218):741–4.

944 15. Brechbiel JL, Gavis ER. Spatial regulation of nanos is required for its function in dendrite
945 morphogenesis. Curr Biol CB. 2008 May 20;18(10):745–50.

946 16. Menon KP, Andrews S, Murthy M, Gavis ER, Zinn K. The translational repressors Nanos and Pumilio
947 have divergent effects on presynaptic terminal growth and postsynaptic glutamate receptor subunit
948 composition. J Neurosci Off J Soc Neurosci. 2009 Apr 29;29(17):5558–72.

949 17. Ye B, Petritsch C, Clark IE, Gavis ER, Jan LY, Jan YN. Nanos and Pumilio are essential for dendrite
950 morphogenesis in Drosophila peripheral neurons. Curr Biol CB. 2004 Feb 17;14(4):314–21.

951 18. Coux RX, Teixeira FK, Lehmann R. L(3)mbt and the LINT complex safeguard cellular identity in the
952 Drosophila ovary. Dev Camb Engl. 2018 Apr 4;145(7).

953 19. Janic A, Mendizabal L, Llamazares S, Rossell D, Gonzalez C. Ectopic expression of germline genes
954 drives malignant brain tumor growth in Drosophila. Science. 2010 Dec 24;330(6012):1824–7.

955 20. Miles WO, Korenjak M, Griffiths LM, Dyer MA, Provero P, Dyson NJ. Post-transcriptional gene
956 expression control by NANOS is up-regulated and functionally important in pRb-deficient cells. EMBO
957 J. 2014 Oct 1;33(19):2201–15.

958 21. Curtis D, Treiber DK, Tao F, Zamore PD, Williamson JR, Lehmann R. A CCHC metal-binding domain
959 in Nanos is essential for translational regulation. EMBO J. 1997 Feb 17;16(4):834–43.

960 22. Weidmann CA, Qiu C, Arvola RM, Lou TF, Killingsworth J, Campbell ZT, et al. Drosophila Nanos acts
961 as a molecular clamp that modulates the RNA-binding and repression activities of Pumilio. eLife.
962 2016 Aug 2;5:e17096.

963 23. Sonoda J, Wharton RP. Recruitment of Nanos to hunchback mRNA by Pumilio. Genes Dev. 1999
964 Oct 15;13(20):2704–12.

965 24. Wang C, Dickinson LK, Lehmann R. Genetics of nanos localization in Drosophila. Dev Dyn Off Publ
966 Am Assoc Anat. 1994 Feb;199(2):103–15.

967 25. Wharton RP, Sonoda J, Lee T, Patterson M, Murata Y. The Pumilio RNA-binding domain is also a
968 translational regulator. Mol Cell. 1998 May;1(6):863–72.

969 26. Arvola RM, Weidmann CA, Tanaka Hall TM, Goldstrohm AC. Combinatorial control of messenger
970 RNAs by Pumilio, Nanos and Brain Tumor Proteins. RNA Biol. 2017 Nov 2;14(11):1445–56.

971 27. Gerber AP, Luschnig S, Krasnow MA, Brown PO, Herschlag D. Genome-wide identification of
972 mRNAs associated with the translational regulator PUMILIO in Drosophila melanogaster. Proc Natl
973 Acad Sci U S A. 2006 Mar 21;103(12):4487–92.

974 28. Laver JD, Li X, Ray D, Cook KB, Hahn NA, Nabeel-Shah S, et al. Brain tumor is a sequence-specific
975 RNA-binding protein that directs maternal mRNA clearance during the Drosophila maternal-to-zygotic
976 transition. Genome Biol. 2015 May 12;16(1):94.

977 29. Lykke-Andersen J, Shu MD, Steitz JA. Communication of the position of exon-exon junctions to the
978 mRNA surveillance machinery by the protein RNPS1. Science. 2001 Sep 7;293(5536):1836–9.

979 30. Nott A, Le Hir H, Moore MJ. Splicing enhances translation in mammalian cells: an additional function
980 of the exon junction complex. Genes Dev. 2004 Jan 15;18(2):210–22.

981 31. Forrest KM, Clark IE, Jain RA, Gavis ER. Temporal complexity within a translational control element
982 in the nanos mRNA. Dev Camb Engl. 2004 Dec;131(23):5849–57.

983 32. Li Y, Minor NT, Park JK, McKearin DM, Maines JZ. Bam and Bgcn antagonize Nanos-dependent
984 germ-line stem cell maintenance. Proc Natl Acad Sci U S A. 2009 Jun 9;106(23):9304–9.

985 33. Gavis ER, Lehmann R. Localization of nanos RNA controls embryonic polarity. Cell. 1992 Oct
986 16;71(2):301–13.

987 34. Hülskamp M, Pfeifle C, Tautz D. A morphogenetic gradient of hunchback protein organizes the
988 expression of the gap genes Krüppel and knirps in the early Drosophila embryo. Nature. 1990 Aug
989 9;346(6284):577–80.

990 35. Wharton RP, Struhl G. Structure of the Drosophila BicaudalD protein and its role in localizing the
991 posterior determinant nanos. Cell. 1989 Dec 1;59(5):881–92.

992 36. Asaoka M, Hanyu-Nakamura K, Nakamura A, Kobayashi S. Maternal Nanos inhibits Importin-
993 α2/Pendulin-dependent nuclear import to prevent somatic gene expression in the Drosophila
994 germline. PLoS Genet. 2019 May;15(5):e1008090.

995 37. Wharton RP, Struhl G. RNA regulatory elements mediate control of Drosophila body pattern by the
996 posterior morphogen nanos. Cell. 1991 Nov 29;67(5):955–67.

997 38. Huang DW, Sherman BT, Lempicki RA. Systematic and integrative analysis of large gene lists using
998 DAVID bioinformatics resources. Nat Protoc. 2009;4(1):44–57.

999 39. Huang DW, Sherman BT, Lempicki RA. Bioinformatics enrichment tools: paths toward the
1000 comprehensive functional analysis of large gene lists. Nucleic Acids Res. 2009 Jan;37(1):1–13.

1001 40. Wu D, Smyth GK. Camera: a competitive gene set test accounting for inter-gene correlation. Nucleic
1002 Acids Res. 2012 Sep 1;40(17):e133.

1003 41. Wharton TH, Marhabaie M, Wharton RP. Significant roles in RNA-binding for the amino-terminal
1004 domains of Drosophila Pumilio and Nanos. 2023; BioRxiv

1005 42. Flora P, Wong-Deyrup SW, Martin ET, Palumbo RJ, Nasrallah M, Oligney A, et al. Sequential
1006 Regulation of Maternal mRNAs through a Conserved cis-Acting Element in Their 3' UTRs. Cell Rep.
1007 2018 Dec 26;25(13):3828-3843.e9.

1008 43. Bailey TL. DREME: motif discovery in transcription factor ChIP-seq data. Bioinforma Oxf Engl. 2011
1009 Jun 15;27(12):1653–9.

1010 44. Kim-Ha J, Kerr K, Macdonald PM. Translational regulation of oskar mRNA by bruno, an ovarian RNA-
1011 binding protein, is essential. Cell. 1995 May 5;81(3):403–12.

1012 45. Reveal B, Garcia C, Ellington A, Macdonald PM. Multiple RNA binding domains of Bruno confer
1013 recognition of diverse binding sites for translational repression. RNA Biol. 2011 Dec;8(6):1047–60.

1014 46. Bansal P, Madlung J, Schaaf K, Macek B, Bono F. An Interaction Network of RNA-Binding Proteins
1015 Involved in Drosophila Oogenesis. Mol Cell Proteomics MCP. 2020 Sep;19(9):1485–502.

1016 47. Sonoda J. Combinatorial Translational Regulators in Drosophila [Ph.D.]. [Durham, NC]: Duke
1017 University; 2001.

1018 48. Verrotti AC, Wharton RP. Nanos interacts with cup in the female germline of Drosophila. Dev Camb
1019 Engl. 2000 Dec;127(23):5225–32.

1020 49. Tadros W, Goldman AL, Babak T, Menzies F, Vardy L, Orr-Weaver T, et al. SMAUG is a major
1021 regulator of maternal mRNA destabilization in Drosophila and its translation is activated by the PAN
1022 GU kinase. Dev Cell. 2007 Jan;12(1):143–55.

1023 50. Eichhorn SW, Subtelny AO, Kronja I, Kwasnieski JC, Orr-Weaver TL, Bartel DP. mRNA poly(A)-tail
1024 changes specified by deadenylation broadly reshape translation in Drosophila oocytes and early
1025 embryos. eLife. 2016 Jul 30;5:e16955.

1026 51. Dalby B, Glover DM. Discrete sequence elements control posterior pole accumulation and
1027 translational repression of maternal cyclin B RNA in Drosophila. EMBO J. 1993 Mar;12(3):1219–27.

1028 52. Tautz D. Regulation of the Drosophila segmentation gene hunchback by two maternal morphogenetic
1029 centres. Nature. 1988 Mar 17;332(6161):281–4.

1030 53. Lott SE, Villalta JE, Schroth GP, Luo S, Tonkin LA, Eisen MB. Noncanonical compensation of zygotic
1031 X transcription in early Drosophila melanogaster development revealed through single-embryo RNA-
1032 seq. PLoS Biol. 2011 Feb 8;9(2):e1000590.

1033 54. Pekovic F, Rammelt C, Kubíková J, Metz J, Jeske M, Wahle E. RNA binding proteins Smaug and
1034 Cup induce CCR4-NOT-dependent deadenylation of the nanos mRNA in a reconstituted system.
1035 Nucleic Acids Res. 2023 May 8;51(8):3950–70.

1036 55. Peng Y, Gavis ER. The Drosophila hnRNP F/H homolog Glorund recruits dFMRP to inhibit nanos
1037 translation elongation. Nucleic Acids Res. 2022 Jul 8;50(12):7067–83.

1038 56. Forbes A, Lehmann R. Nanos and Pumilio have critical roles in the development and function of
1039 Drosophila germline stem cells. Dev Camb Engl. 1998 Feb;125(4):679–90.

1040 57. Parisi MJ, Deng W, Wang Z, Lin H. The arrest gene is required for germline cyst formation during
1041 Drosophila oogenesis. Genes N Y N 2000. 2001 Apr;29(4):196–209.

1042 58. de Cuevas M, Lee JK, Spradling AC. alpha-spectrin is required for germline cell division and
1043 differentiation in the Drosophila ovary. Dev Camb Engl. 1996 Dec;122(12):3959–68.

1044 59. Lin H, Yue L, Spradling AC. The Drosophila fusome, a germline-specific organelle, contains
1045 membrane skeletal proteins and functions in cyst formation. Dev Camb Engl. 1994 Apr;120(4):947–
1046 56.

1047 60. Röper K, Brown NH. A spectraplakin is enriched on the fusome and organizes microtubules during
1048 oocyte specification in Drosophila. Curr Biol CB. 2004 Jan 20;14(2):99–110.

1049 61. Signer RAJ, Magee JA, Salic A, Morrison SJ. Haematopoietic stem cells require a highly regulated
1050 protein synthesis rate. Nature. 2014 May 1;509(7498):49–54.

1051 62. Nakatani T, Lin J, Ji F, Ettinger A, Pontabry J, Tokoro M, et al. DNA replication fork speed underlies
1052 cell fate changes and promotes reprogramming. Nat Genet. 2022 Mar;54(3):318–27.

1053 63. Laver JD, Marsolais AJ, Smibert CA, Lipshitz HD. Regulation and Function of Maternal Gene
1054 Products During the Maternal-to-Zygotic Transition in Drosophila. Curr Top Dev Biol. 2015;113:43–
1055 84.

1056 64. Tautz D, Pfeifle C. A non-radioactive in situ hybridization method for the localization of specific RNAs
1057 in Drosophila embryos reveals translational control of the segmentation gene hunchback.
1058 Chromosoma. 1989 Aug;98(2):81–5.

1059 65. Edgar BA, Sprenger F, Duronio RJ, Leopold P, O'Farrell PH. Distinct molecular mechanism regulate
1060 cell cycle timing at successive stages of Drosophila embryogenesis. Genes Dev. 1994 Feb
1061 15;8(4):440–52.

1062 66. James P, Halladay J, Craig EA. Genomic libraries and a host strain designed for highly efficient two-
1063 hybrid selection in yeast. Genetics. 1996 Dec;144(4):1425–36.

1064 67. Hook B, Bernstein D, Zhang B, Wickens M. RNA-protein interactions in the yeast three-hybrid
1065 system: affinity, sensitivity, and enhanced library screening. RNA N Y N. 2005 Feb;11(2):227–33.

1066

1067

1068 **Supporting Information**

1069

1070 **S1 Fig.** Multi-dimensional scaling plot of RNAseq data in Fig 2.

1071 **S2 Fig.** Smear plots of the RNAseq data plotted for individual mRNAs rather than

1072 gene-binned mRNAs (as in Fig 2A).

1073 **S3 Fig.** Boxplot showing that mRNAs targeted by Upf1-Nos have, on average, slightly

1074 shorter 3'-UTRs than non-targeted mRNAs.

1075 **S4 Fig.** Barcode plot showing no significant enrichment of mRNAs targeted by Upf1-
1076 Nos among Bru-repressed mRNAs.

1077 **S1 Data.** Data for Fig 1.

1078 **S2 Data.** Data for Fig 2.

1079 **S3 Data.** Data and statistical analysis for Fig 4.

1080 **S4 Data.** Data and statistical analysis for Fig 5.

1081 **S5 Data.** Data and statistical analysis for Fig 6.

1082 **S6 Data.** Plasmids used in this work.

1083

1084

1085

1086

1087

Upf1-Nos fig 1

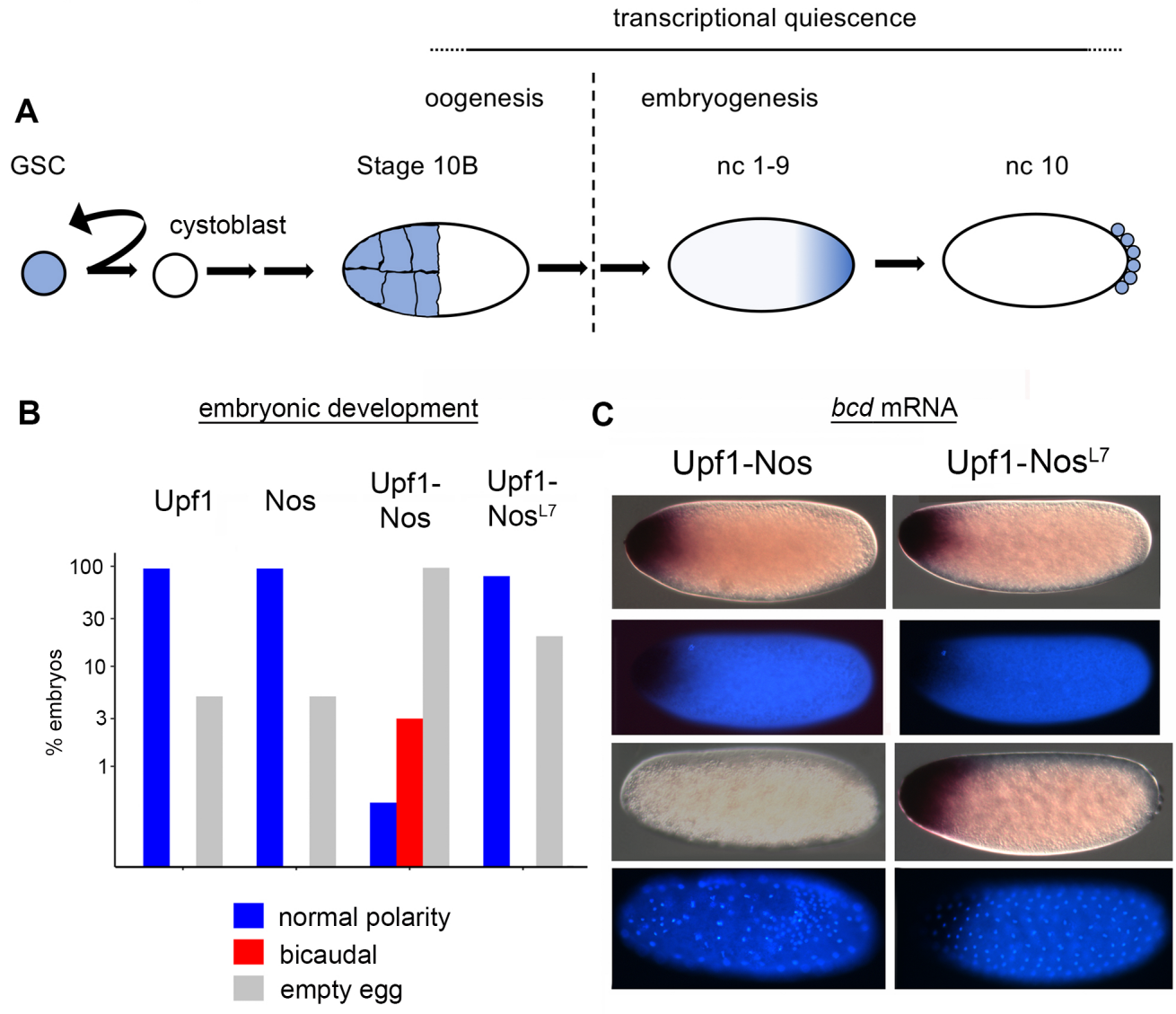

Upf1-Nos fig 2

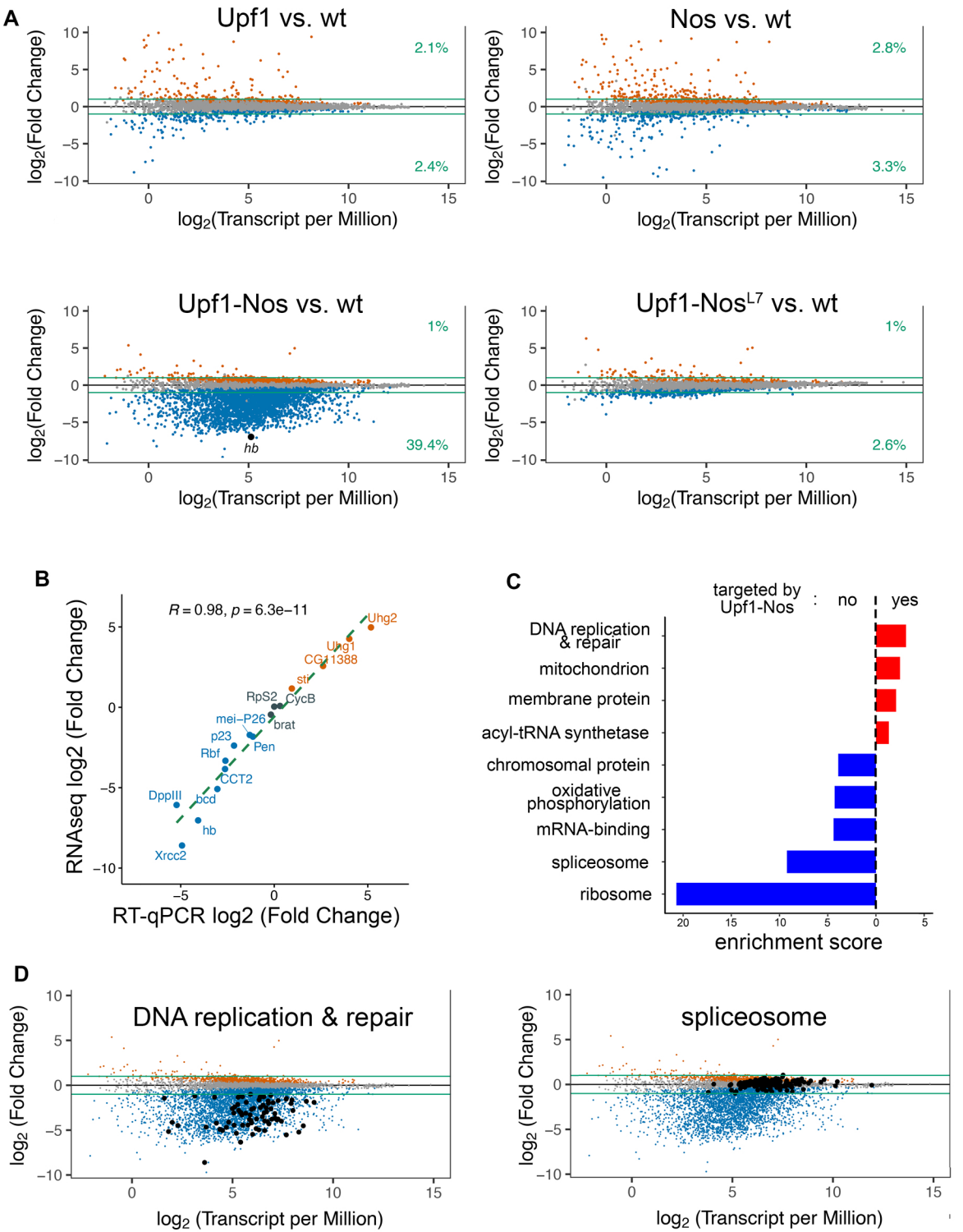

Upf1-Nos fig 3

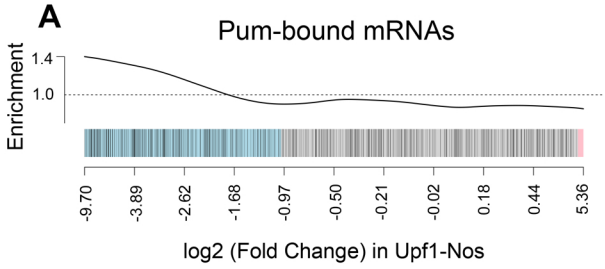

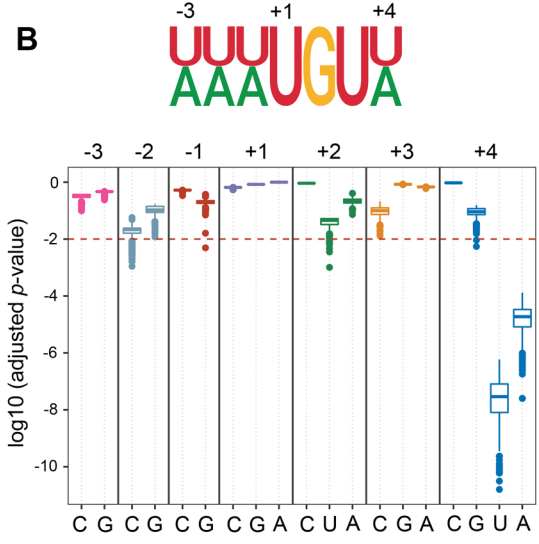

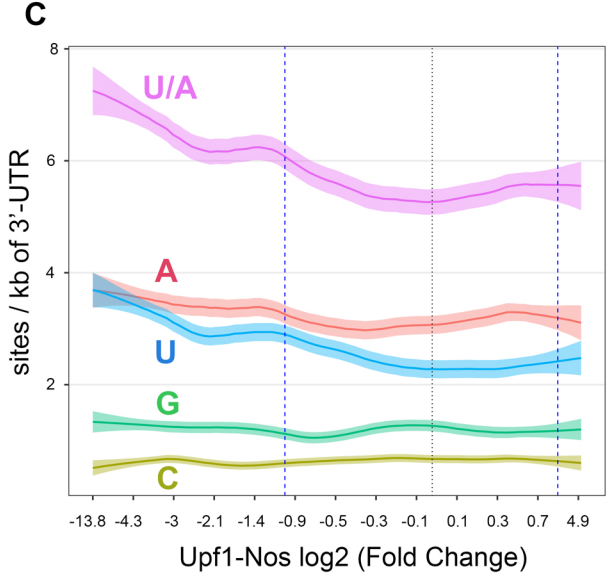

Upf1-Nos fig 4

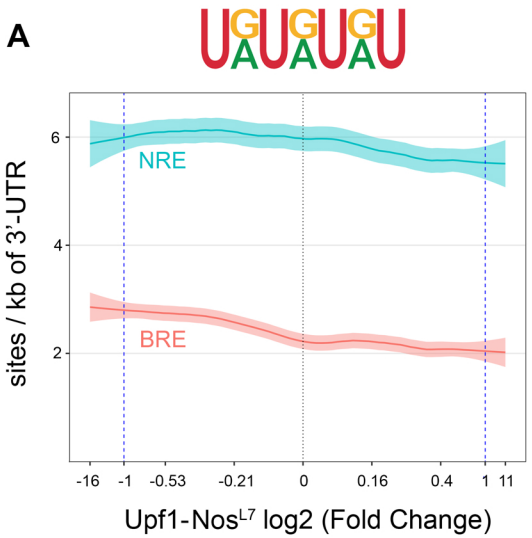

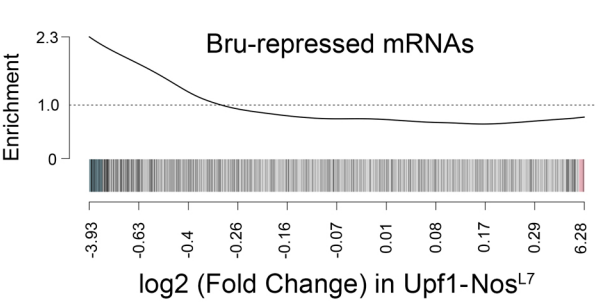

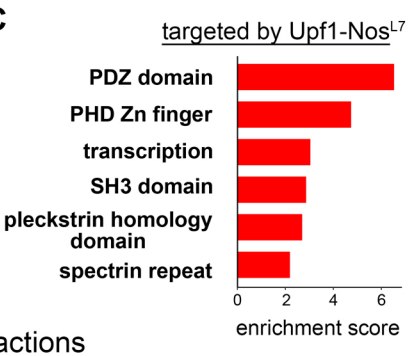

Nos-Bru interactions

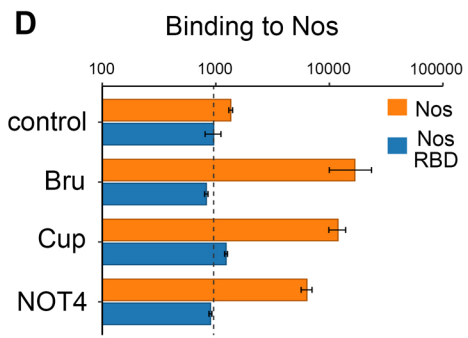

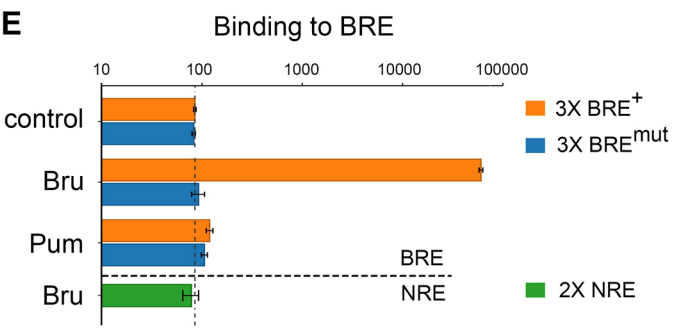

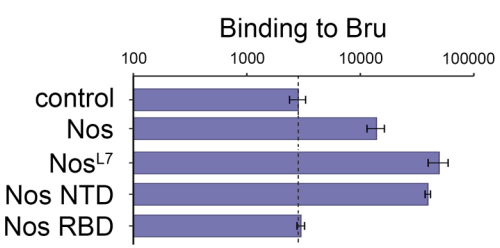

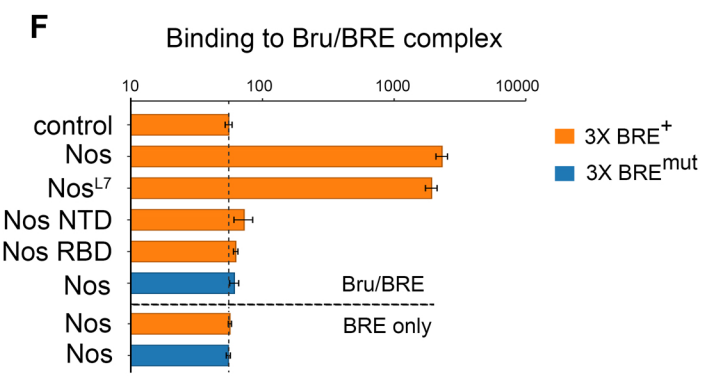

Upf1-Nos fig 5

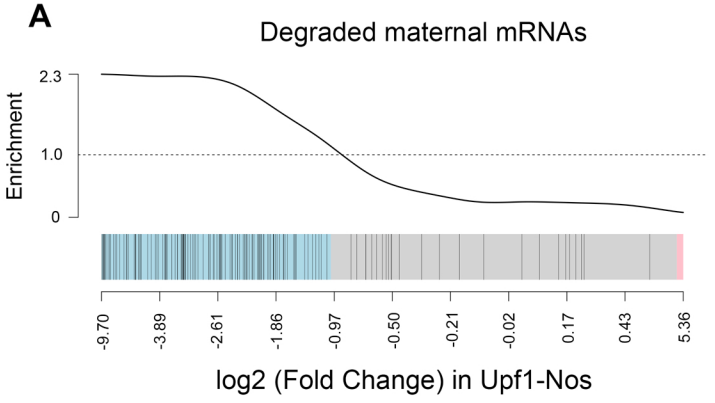

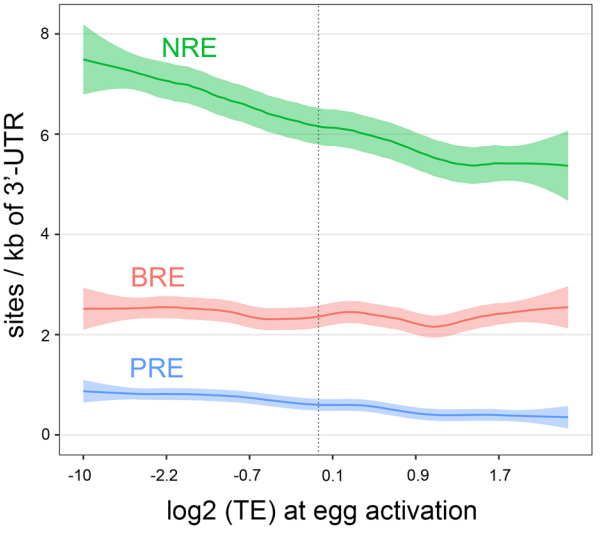

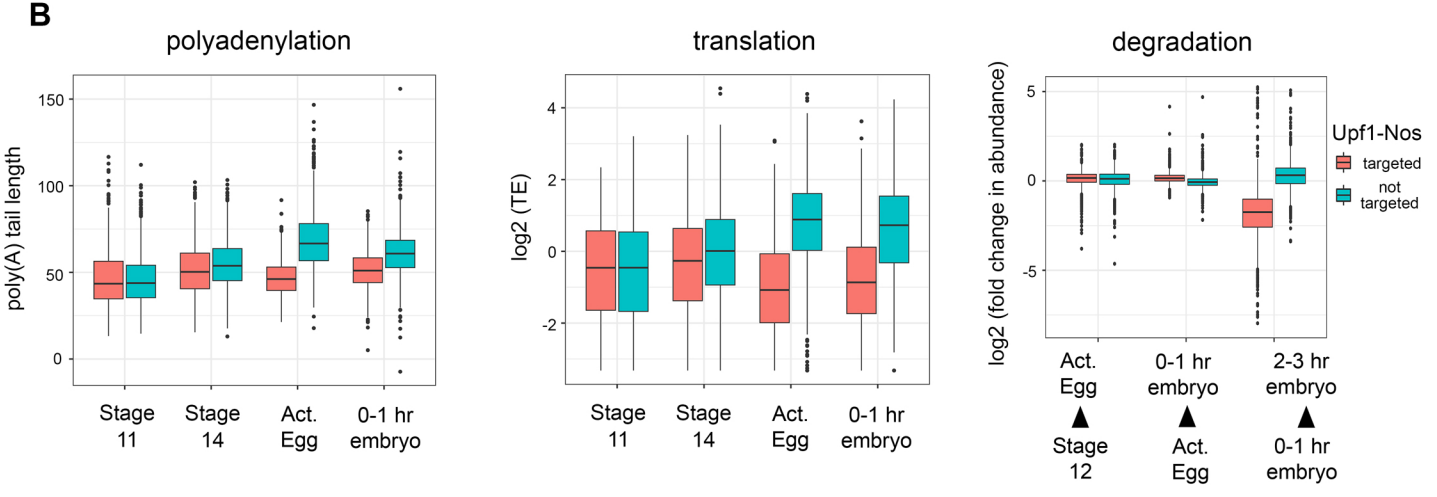

Upf1-Nos fig 6

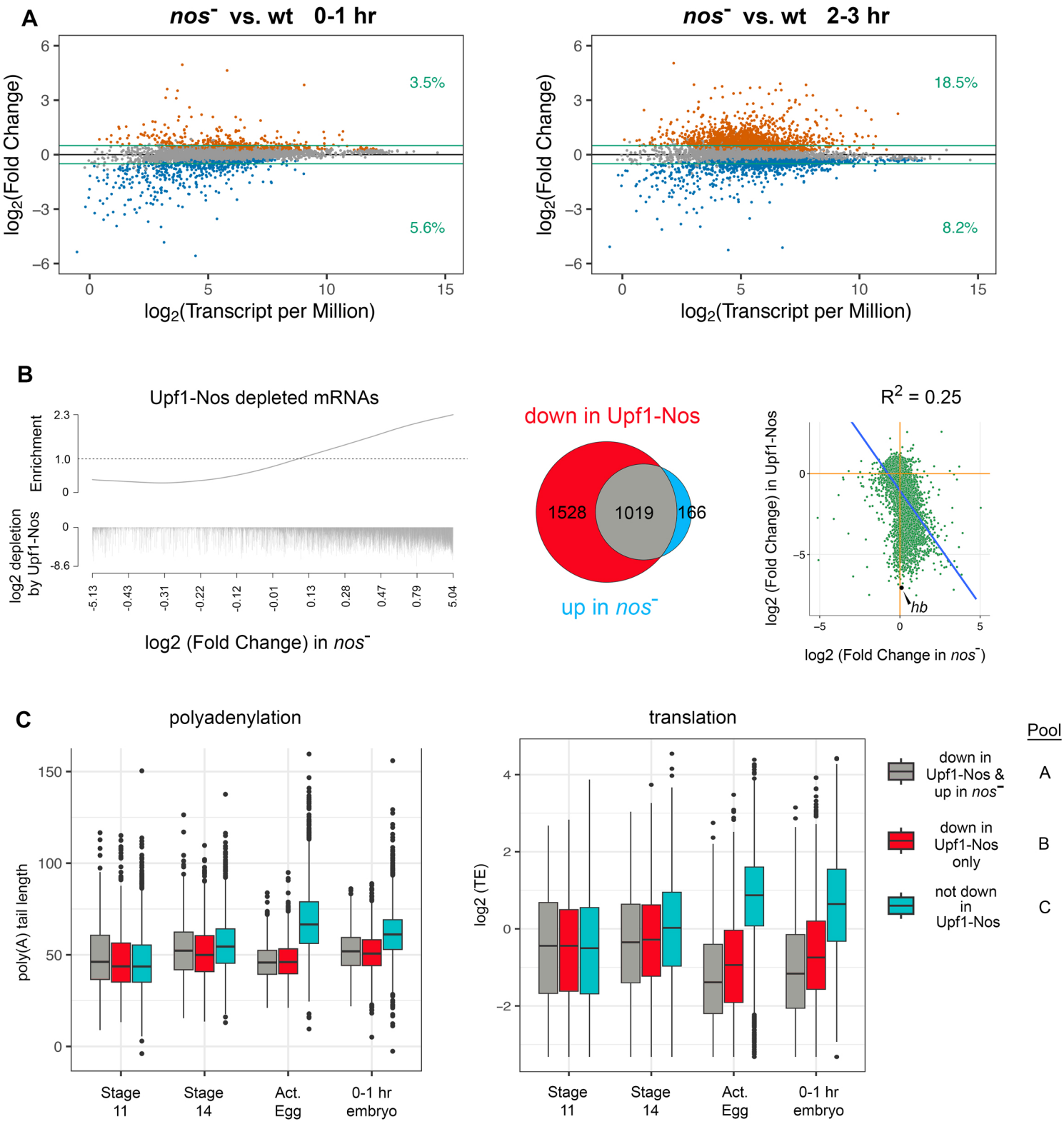

Upf1-Nos Supplementary Figure 1

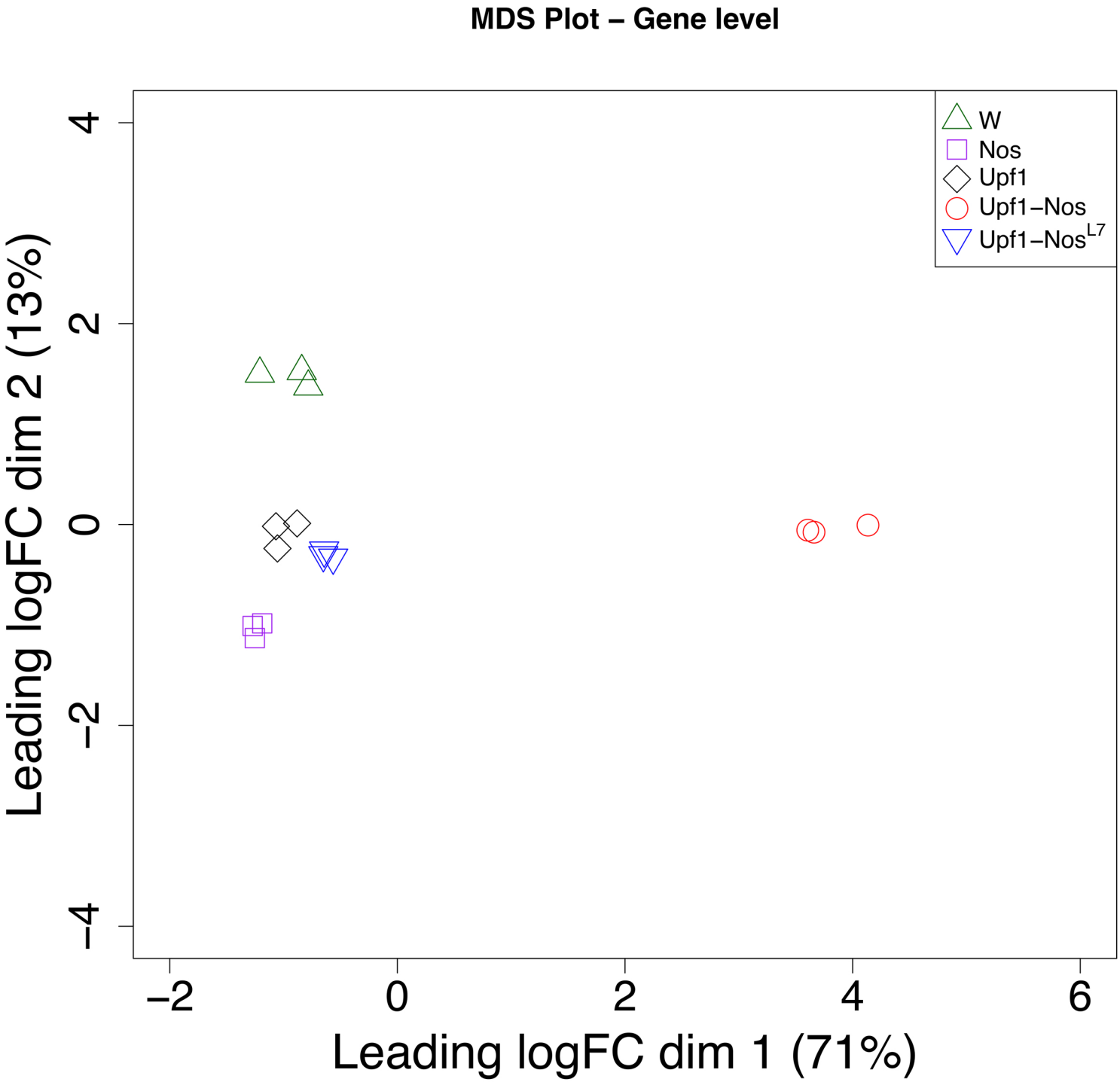

Upf1-Nos Supplementary Fig 2

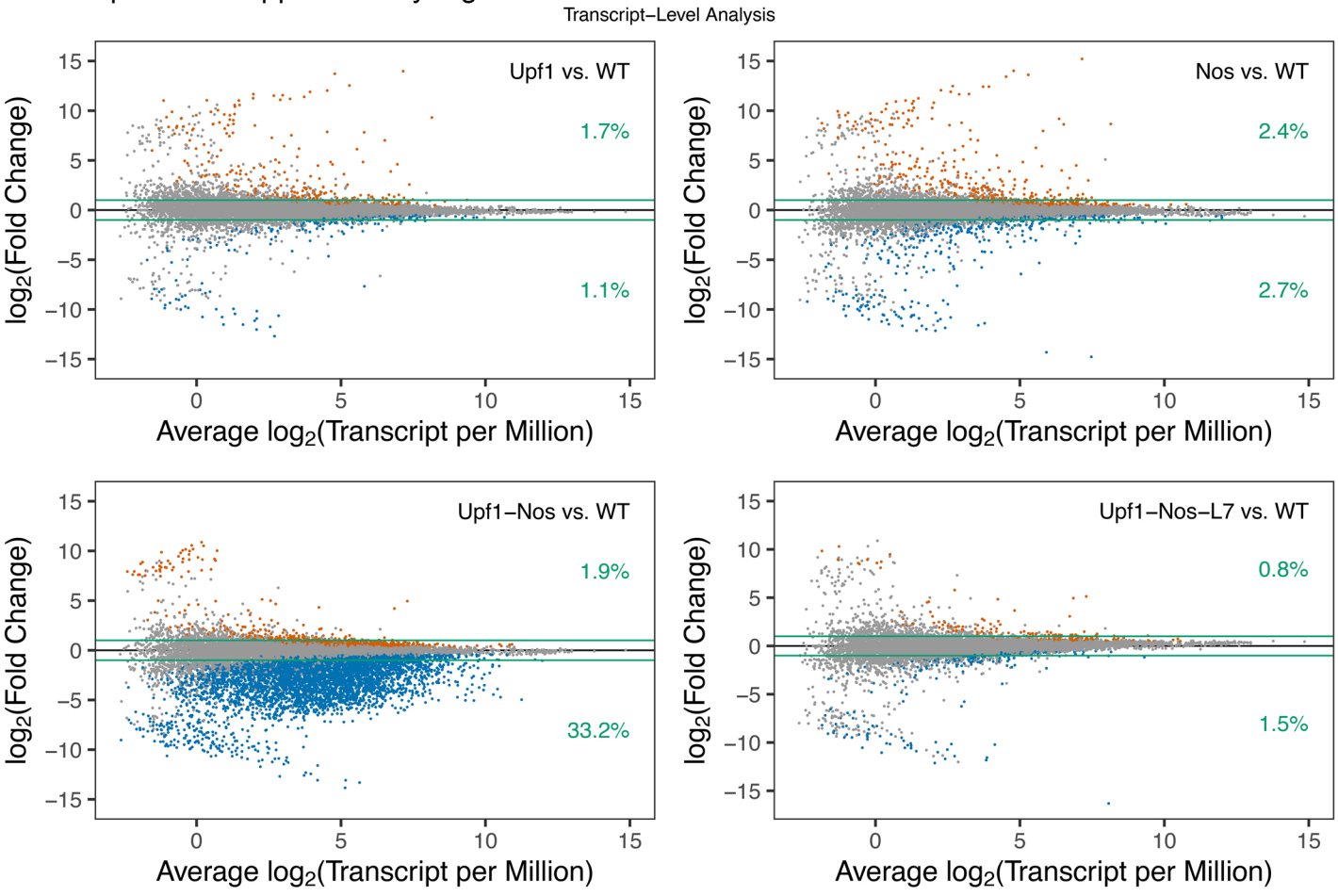

Upf1-Nos Supplementary Fig 3

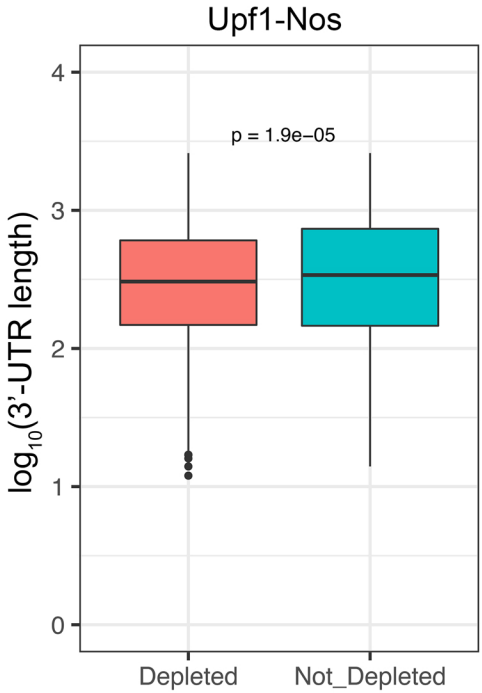
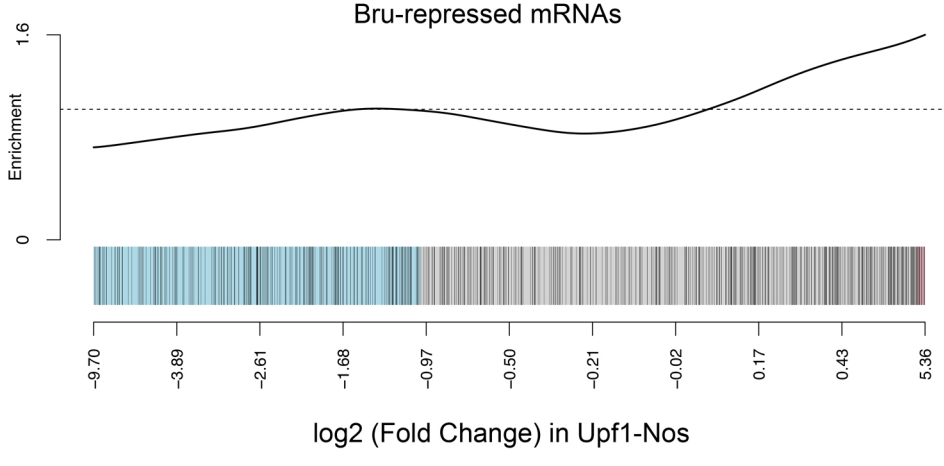
Upf1-Nos Supplementary Fig 4